Master Thesis College of Human Ecology

Preparation of superhydrophobic cotton fabric from waterborne Octadecylamine / alkyl silane coating

(옥타데실아민/알킬 실레인 수분산 코팅을 통한 초소수성 면 직물 개발)

August, 2018

Department of Textiles, Merchandising, and Fashion Design

The Graduate School of Seoul National University

MD ASHIKUR RAHMAN

라만

ABSTRACT

In this study, it was aimed to develop a simple way to design durable multifunctional superhydrophobic cotton surface by using self-assembled ODA layer to support formation of nanostructure with HDTMS in using aqueous dispersion.

To examine the effect of ODA and HDTMS concentration, the morphology and the chemical composition were investigated according to molar ratios. The surface morphology was investigated by Field Emission Scanning microscope (FE-SEM) with high magnification (nanometer scale). The Chemical compositions were examined by Fourier-transform infrared spectroscopy (FT-IR) and X-ray photoelectron spectrophotomer (XPS) to confirm coating materials were successfully coated on the fiber surface. Surface wettability was evaluated by static contact angle and shedding angle using distilled water. Functional durability, self-healing properties and breathability were also investigated.

When cotton fabric was coated by only ODA micro-nano roughness was not formed (CA=0º) because ODA dissolved in water. But when cotton fabric was coated by HDTMS, surface become hydrophobic (CA=148º, SA=17º) and micro-nano roughness was formed. Interestingly, when cotton fabric dipped into ODA/HDTMS mixed solution micro-nano scale roughness was formed. At concentration ranging ODA/HDTMS 3:1 to 1:2 molar ratio surface became rougher

thus changing water contact angle higher than 150º and water shedding angle below 10° was achieved respectively. The best superhydrophobicity was recorded at 1:2 ODA/HDTMS molar ratio as highest static contact angle, WCA 161.4± 1.6° and water shedding angle, WSA lowest as WSA 8.5± 0.7° .

The contribution of this study is that superhydrophobic coating was applied via simple one step dip coating method of reducing surface energy and forming micro-nano scale roughness at the same time in aqueous system.

Keyword: Superhydrophobicity, Self-healing, Non-flouro materials, Biosilicification, Dip-coating

Student ID: 2016-26765

CONTENTS

List of figures

List of schemes and tables

Chapter 1. Introduction

1. Purpose

Recently, superhydrophobic surface has become one of the key research area in textile especially in advanced textile finishing and other fields due to its superb diverse application and multifunctional properties. And various methods are used to design superhydrophobic surface by combination of changing surface roughness scale and surface energy such as plasma deposition [1], chemical vapor deposition [2], nano particles deposition [3], sol-gel methods etc. [4]. Superhydrophobic multifunction properties such as self-cleaning properties can keep product dust free even without washing used in footwear and daily life products. [5-6]. Oil water separation in deep sea when oil split occurs [7]. anti-fogging, anti-fouling used in automobile and marine industry [8], anti-icing well known in air plane manufacturing industry [9]. Some other non-textile applications are drug reduction, anticorrosion, construction materials, microfluids device, smart windows, etc. [10-14]

It is concise that superhydrophobicity can be formed when lowering surface energy lower than water when surface became macro-nano scale roughness. Superhydrophobic surface exhibits water contact angle higher than 150° and water drops shedding angle below 10°. Preparing superhydrophobic surface designed by using fluorine

containing substances and fluoro containing materials highly environment unfriendly due to bio-accumulations and have been restricted for application in fabric finishing. So, fluorine-free superhydrophobic coating materials are highly recommended.

In recent years, fluorine-free superhydrophobic treatments are studied by several research groups such as facile fabrication of superhydrophobic SiO_2 and polystyrene coating by using different solution systems [15] polydimethylsiloxane (PDMS) solution containing onion-like carbon microspheres [16], and PDMS containing graphene oxide [17]. But some of these works involved few organic solvents which are highly toxic, non-ecofriendly also may high cost. So superhydrophobic fabrics prepared by fluorine-free solvents like water is highly desirable. Recently, few reports on waterborne superhydrophobic surface by using various methods [18-21]. In most of the cases, functional durability, surface compatibility, complicated preparation process, cost, and non-repairable character superhydrophobic surface limit to large scale production thus restrict the use of such surface in real life applications [22]. Therefore, fabrication of waterborne, fluorine-free superhydrophobic surface with durable and self-cleaning properties is highly desirable.

ODA is known as a low surface energy material and widely used to fabricate self-healing superhydrophobic surfaces based on the migration of ODA molecules [23-26], ODA, having long-chain

amphiphilic alkyl amine, widely used in the Langmuir–Blodgett technique as a template [27]. The hydrolytic polycondensation of organosilanes in solution produce micelle formation with a mixture of cages, ladder like, petals or network structure [28].

HDTMS is an organosilane with siloxane functional group. Silicones are widely used in biomedical and cosmetics due to its toxicity has been extremely examined. In addition, silanes are also used in surface modification to lowering surface energy due to its safety and environment considerations. HDTMS can easily make Si–O–Si bonding with cotton cellulose by hydrolysis or polycondensation through hydroxyl groups at room temperature.

In this study, superhydrophobic fabric has been prepared by simple coating of fluorine–free, ODA and HDTMS through aqueous system. We utilized, a self–assembled micro–nano structured ODA layer as a catalyst to support formation of petals by HDTMS hydrolytic polycondensation of organosilanes. The surface with micro–nano structure and morphology of ODA/HDTMS coating surface were adjusted by changing ODA/HDTMS molar ratio in the coating solution. Surface morphology, surface chemical compositions, anti–wettability, durability, self–healing properties and breathability are investigated with different ODA/HDTMS molar ratio.

2. Theoretical background

2.1 Superhydrophobicity

The term ‘hydrophobicity’ meaning interpretation is that property of materials getting least wetting in nature and superhydrophobicity reveals which are extremely anti-wetting or difficult to wet. These properties have maximum tendency to repel water from the surfaces. Natural phenomena superhydrophobicity first observed by Germen biologist Barthlott and Neihuis in 1997. They conducted by them in depth research that such characteristics was resulted from the joint action of the micron-scale mastoids and hydrophobic waxiness [29] results through ‘Self-cleaning of biological surfaces’. The lotus leaf surface has self-cleaning properties and extreme anti-wetting effect, as contact angle was 160.4 ± 0.7°, and the shedding angle is 1.7° These unique properties take away the contamination from the surface that known as ‘lotus effect’ (Figure 1-c). Later on Cao et al. [30] reported improved view of Barthlott and Neihuis and they contemplated that the surface roughness of the lotus leaf was not only resulted from the action of micron-scale actually, there existed mastoid of micron-size, and such combination of micro-nano structure served root cause of superhydrophobic surface. The SEM photograph of the mastoids on the lotus leaf surface is shown in Figure1-(d), each of which was composed of nanostructure branches with average diameter of 120-130nm. But self-cleaning

characteristics in nature not only found in lotus leaf but Some other plants and insects found self−cleaning surfaces such as Rice leaves, Salvinia molesta, butterfly wings fish scales, shark skin and mosquito eyes etc. (Figure 2) [31−32].

Such natural bio−surface have attained attention from both industrial and academic researchers due to its potential application and multifunction properties example as self−cleaning, water repellency, oil water separation, anti−corrosion, anti−fogging, anti−icing (for road, aircrafts, power line), antifouling and anti− bacterial properties etc.

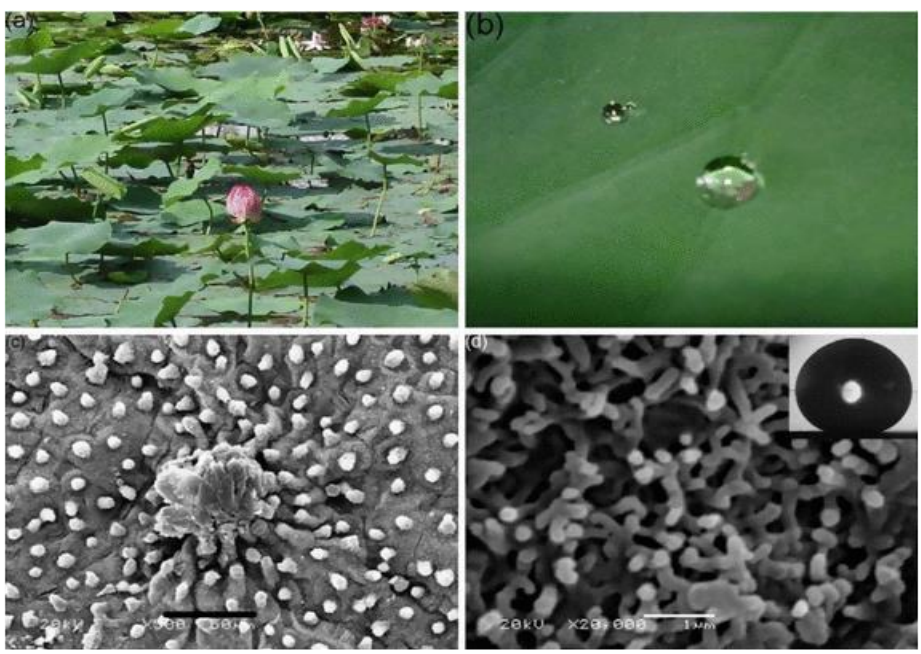

Figure 1(a). The photos of some lotus leaf (b) a water droplet on a lotus leaf (c and d) SEM image of lotus leaves with different magnifications, (c). The inset of (d) is a water contact angle on a lotus leaf 161° ±2° .

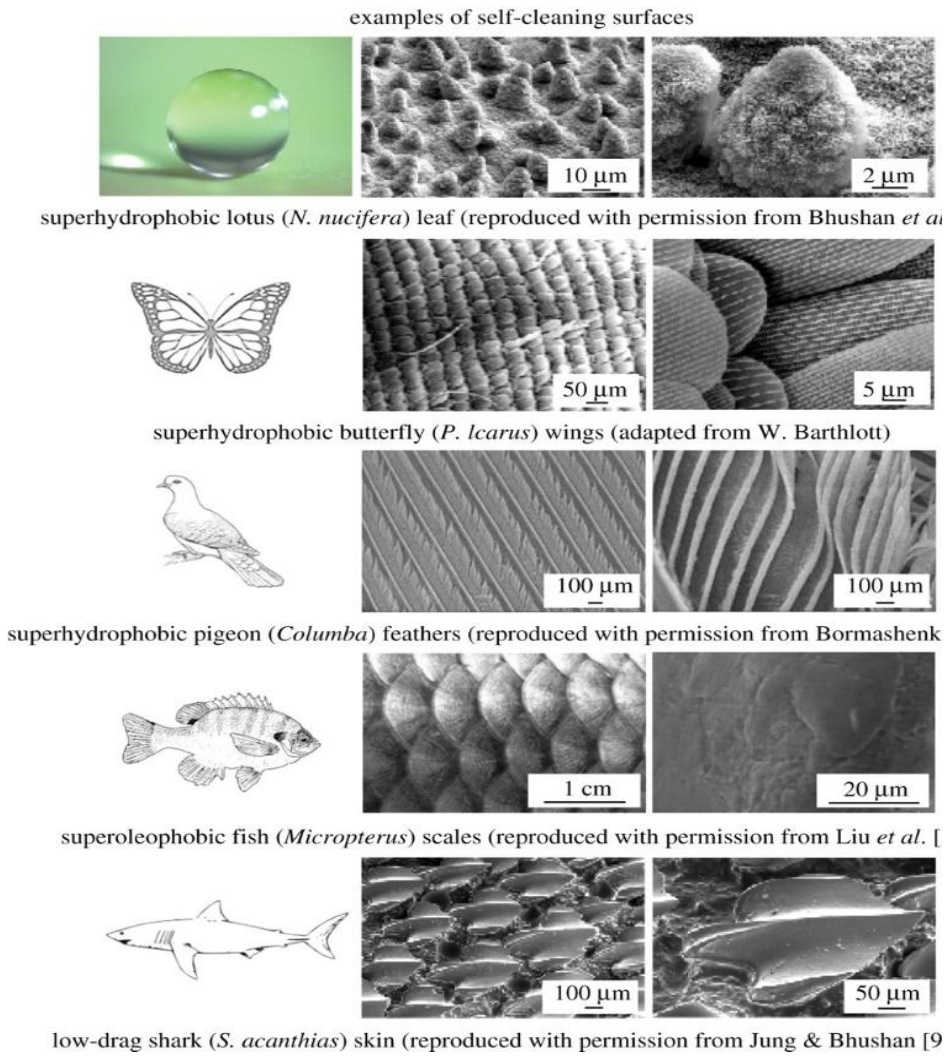

Figure 2. Self-cleaning surface in nature (Re-print from refn.31)

2.1.1 Wetting behavior on smooth solid and rough solid surface

There are three main fundamental theories that explain the wettability of a solid surface. Assuming a smooth solid surface that explain by Young's theory [33] and assumes rough solid surfaces, Wenzel [34], Cassie–Baxter theory [35] can be theoretically calculate the contact angle of a drop.

Young's theory

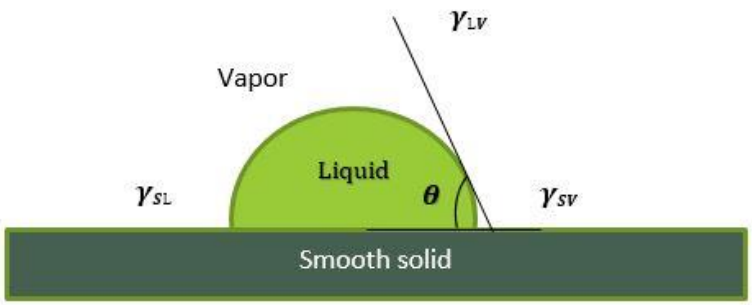

Figure 3. Schematic diagram of a static contact angle of liquid droplet on a smooth surface: Young's theory [21].

$$\gamma_{SV} = \gamma_{SL} + \gamma_{LV} \cos \theta \qquad (1)$$

Where, θ is Static contact angle; γ_{SV} is the solid−vapor interfacial energy; γ_{SL} is the solid−liquid interfacial energy and γ_{LV} is the liquid−vapor interfacial energy.

Young [33] has shown that the wettability on flat, chemically uniform ideal solid surfaces. As shown in equation (1), the relationship between the static contact angle and the interfacial energy between solid−liquid and gas. The surface tension γ_{LV} of the liquid and the interfacial tension γ_{SL} of the solid and liquid are large, When the surface energy (γ_{SV}) of the solid is small, the cos θ value becomes small, and the θ value becomes large, so that the liquid does not wet the solid surface well. In Young's theory, only γ_{LV} can be measured experimentally, by using contact angle measurements, including capillary rise and pendant drop. But no explanation to measure γ_{SV} and γ_{SL} separately. The Young's equation is used only for smooth surface, but when the surface become rough, the Young's equation not work. So later on Wenzel in 1936[34] and then by Cassie and Baxter in 1944[35] discussed roughness factor can strongly affect the wetting of a surface.

Wenzel’ s Model

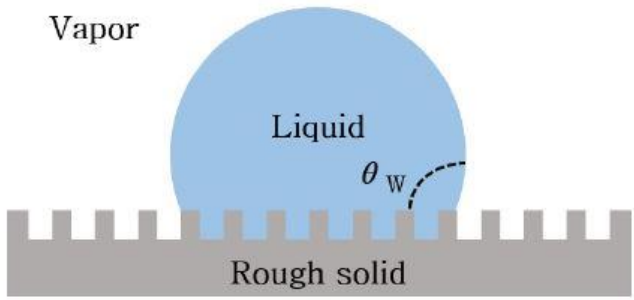

Figure 4. Schematic diagram of a static contact angle of liquid droplet on a rough surface: Wenzel model [34].

$$\cos \theta_W = r \cos \theta \qquad (2)$$

Where, θ is static contact angle at smooth surface; θ_W is static contact angle on rough surface; **r** is roughness constant (actual contact area between liquid and solid / projected area of liquid drop)

Wenzel [34] reported that the contact angle at the surface where the roughness exists is flat

that it is proportional to the contact angle and the roughness constant (r). In Wenzel theory, the roughness constant r is defined as the area of the liquid droplet projected and the actual represented by the ratio of contact area. However, when the droplet is in complete contact with the solid surface the roughness constant r always has a value larger than 1 (as equation 2) Because of this, on a hydrophilic surface

when θ value less than 90° as the roughness increases, the contact angle decreases and on a hydrophobic surface when θ value more than 90° as the roughness increases, the contact angle also increases.

Cassie–Baxter model

In the theory of Cassie–Baxter [35], the droplet is in complete contact with the rough solid surface instead, the solid surface, and the trapped air between the solid and liquid, respectively (as figure 5) is assumed to be in contact with each other.

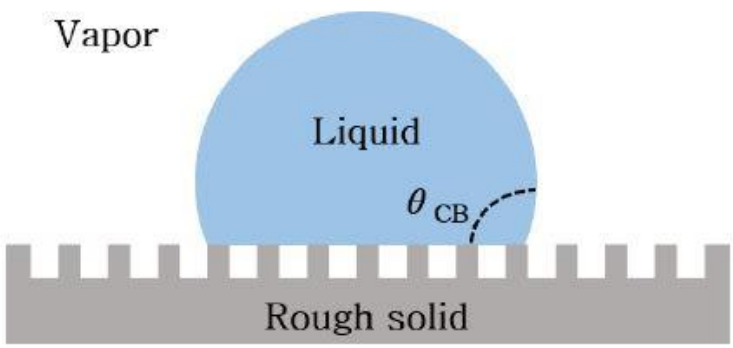

Figure 5. Schematic diagram of a static contact angle of liquid droplet on a rough surface: Cassie–Baxter model [35].

$$\cos \theta_{CB} = f_s \cos \theta + f_{air} \cos \theta_{air} \qquad (3)$$

Where, θ is static contact angle at smooth surface; θ_{CB} is static contact angle on rough surface; θ_{air} is the static contact angle at the interface between the liquid and the gas; f_s is actual contact area between liquid and solid / projected area of liquid

droplet and f_{air} is actual contact area between liquid and gas / Projected area of droplet.

Cassie impregnating wetting state

Based on the hierarchical micro- and nanostructures on the surface which trap air to support water drops to rise on hydrophobic surface than smooth surface. For the lotus effect, due to hierarchical structure the droplets can easy be rolling off in Cassie-Baxter state than smooth surface [36]. However, the Cassie impregnating wetting state conforming petal effect micro-structure was the main reason for the adherence. Thus, water droplets can wet big gaps among micro-scale structures and large amount of liquid solid contact surface would emerge. So, water droplets can pin on the surface due to high adhesive force. This phenomenon was term as Cassie impregnating wetting state (Figure 6) verified by Feng [37] and Bhushan *et al.* [38]. And Cassie impregnating state can be established as equation 4.

$$\cos\theta^{*} = 1 - f_s + f_s \cos\theta \qquad (4)$$

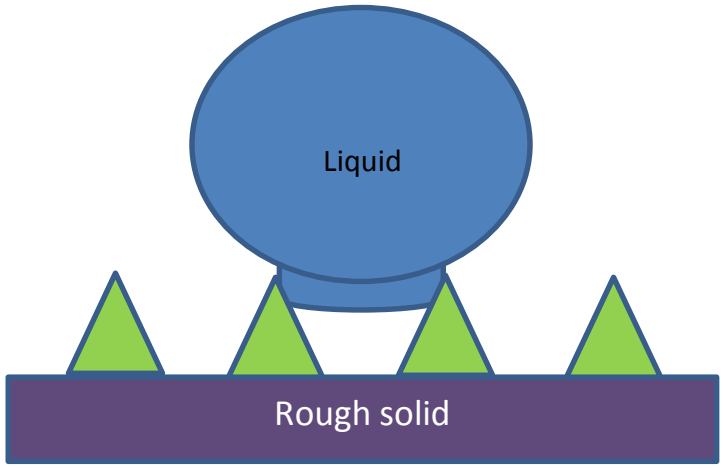

Figure 6. Schematic illustrations of a drop of water in contact with the petal (the Cassie impregnating wetting state)

2.1.2 Contact angle hysteresis (shedding angle)

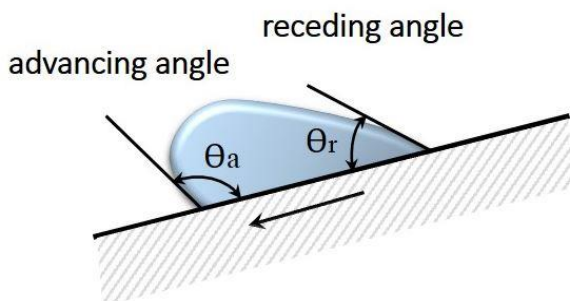

Figure 7. Schematic illustrations of a drop of water in contact with the petal (the Cassie impregnating wetting state)

shedding angle can be defined as minimum tittle angle when droplets starts to slide off, this angle used to characterize the anti-wettability of a solid surface [39]. When increasing of tittle angle (right side angle) advancing angle, θa will be increased, similarly when left side angle increasing receding contact angle θr) will be decreased (As figure 6). When liquid drops start to slide-off, contact angle hysteresis can be calculated as θ (hysteresis) = θa - θr. On rough surface liquid drops has high contact angle hysteresis for example Wenzel's state the shedding angle is generally above 20° and Cassie's state the shedding angle is less than 10°. Cassie impregnating wetting state shedding usually higher up to 90° even higher static contact angle due to its higher adhesive force.

2.2 Approaches to fabricate Superhydrophobicity

2.2.1 Experimental approaches to fabricate superhydrophobic surface

Pioneer research on superhydrophobic surface was done by German biologist of Barthlott and Neihuis from lotus leaf known as 'lotus effect' in 1997. The most well-known lotus surface has self-cleaning in nature with high water contact angle above than 150° and shedding angle below 10°. Researcher conducted that due to complex micro nano roughness on the surface and low surface energy wax, surface showed anti-wetting characteristics on surface. So summary of research is that the combination of dual scale micro-

nano roughness and low surface energy materials minimize the adhesion of water on its surface. According to this mechanism, during last few decays there is plenty of approach to replicate the lotus effect to create superhydrophobic surface. Some of common principles and fabrication methods are described below, challenges of superhydrophobic materials are also briefly discussed.

Templating technique:

Templating is a technique to replicate patterns or shapes of a surface by using polymers. The main purpose is to replicate lotus surface with combination of nano roughness and lower surface energy by suitable materials, polymers by using templating and after curing remove solidified materials from template.

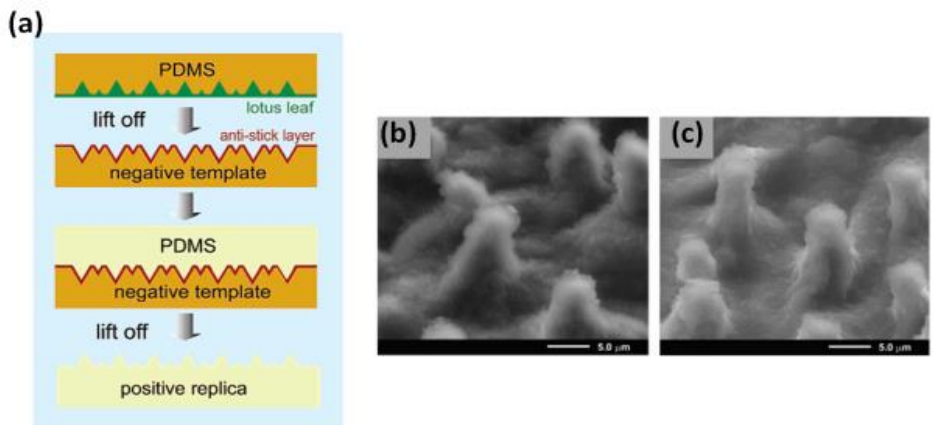

Figure 8. (a) Illustration of the lotus leaf replication process (b) SEM image of natural the lotus leaf (c) its positive replica. Both are almost similar surface morphology. (Reprinted from ref [40])

In 2005, Yong Chen *et al*. templating lotus leaf surface by a PDMS or PMMA polymer solution. After cured and solidification the PDMS layer was removed or peeled off. The roughness of the natural lotus leaf replica was transferred to the negative template. Similarly, PDMS replication template followed in the same procedure SEM images (Figure 7). This template PDMS surface showed high static contact angle above 155° and shedding angle of low than 2° [40]. During last few years, templating is a useful and wide technique to mimic or replicate lotus effect to fabricate superhydrophobic surface. However, with some exceptions like inorganic materials and metals this an easy way to mimic superhydrophobic surface as lotus leaf.

Plasma treatment

Designing superhydrophobic surface by inspired from mimic lotus leaf surface has gain lots of attraction last few decays due to its wide applications. The superhydrophobic surface is defined as measuring static contact angle higher than 150° and shedding lower than 10° by combination of a dual roughness structure with lowered surface energy. The preparation of superhydrophobic surface involved fluoro containing substances and nano particles that issued bio accumulation and affect human heaths. Plasma etching or treatments has potential advantage without any nano particles and chemical involvements that inspired researchers to design superhydrophobic surface. Park *et.al* reported, particle-free, environmental friendly fabrication of

superhydrophobic surface by forming dual-scale roughness and lowering the surface energy via plasma etching and plasma enhanced chemical vapor deposition (PECVD) [41]. They also reported, in the presence of a fabric's microscale roughness, the superhydrophobicity with a contact angle higher than 160° where without nano scale roughness the fabric was not able to exceed static contact angle 144° thus this result corroborates to Young's, Wenzel's, and Cassie-Baxter models.

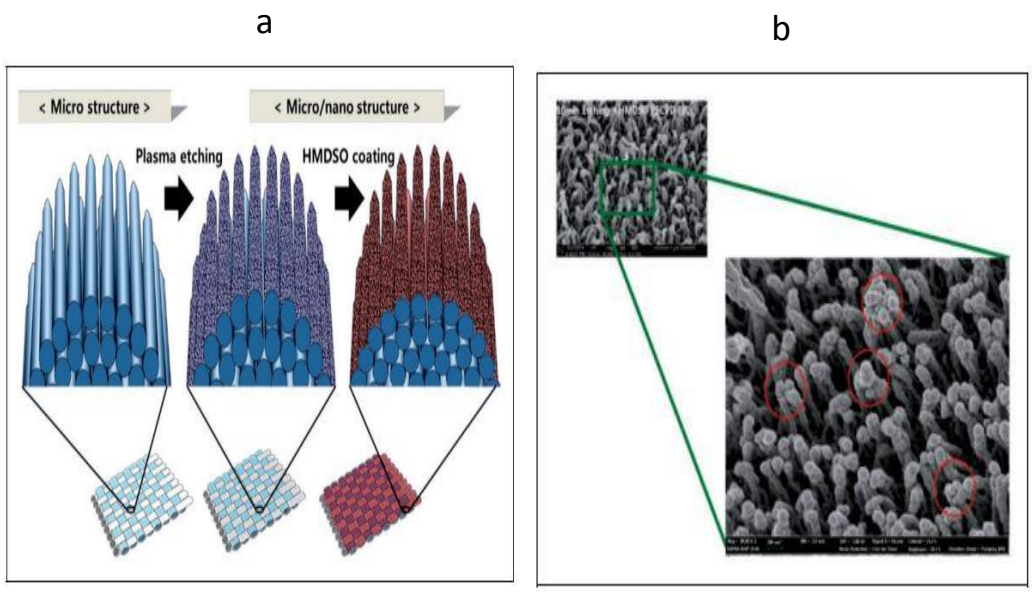

Figure 9. (a) Illustration of micro- and nano-scale dual roughness formed on a fabric, and (b) nano-pillar formation by simple plasma etching and HMDSO coating (Reprinted from refn [41]).

Aggregation/assembly of colloids

Micro-nano roughness can be formed colloidal particles by utilizing Van der Waals forces and electrostatic forces between particles and substrate.

W. Ming *et al* report an easy way to fabricate superhydrophobic films with micro-nano scale structure by raspberry-like particles. The preparation methods are illustrated in figure 10, based on epoxy-amine system by surface grafting. This method involved duel scale roughness, the micro scale roughness formed by large silica particles called raspberry like particles and silica beads contributed nano-scale roughness on the surface. These micro- nano dual scale roughness structures assemble on the surface and showed as lotus leaf. It has static contact angle of 154° and shedding angle less than 3° [42]

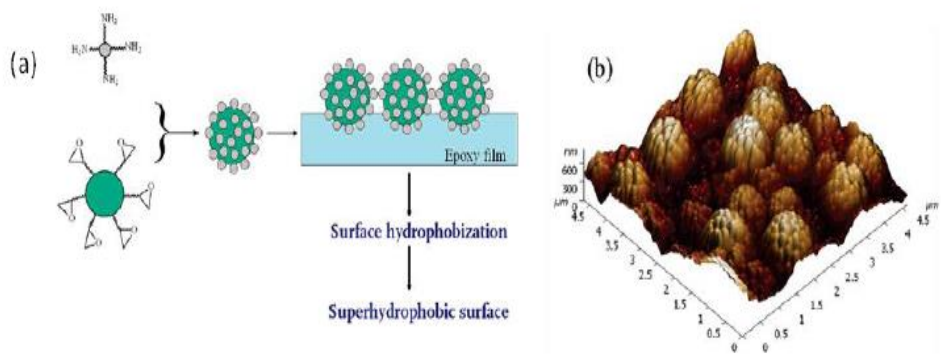

Figure 10. (a) Preparation method of raspberry-like particles (b) AFM 3D images for PDMS-covered epoxy-based film (Reprinted from ref [42])

Biosilicification process

Biosilicification-inspired approach to fabricate superhydrophobic surface by nanofilament coatings using a self-assembled polyamine layer as a template/ catlyst to help formation of one dimentional nanofilament of polysilsesquioxanes by hydrolytic polycondensation of organotrimethoxysilanes. For biomimetic fabrication by coating of polysilsesquioxanes nano-filaments and polyamine self assembled layer formed through cystallization controlled polyethelenimine (LPEI, [NHCH2CH2] backbone) on glass substrate using as template to support hydrolytic polycondensation of organosilanes.

In generally, polysilseequioxanes are chemically and physically more durable with organic polymers and expand mechanical robusness [43]). Such advantages facilities for applications of PSQ based soft nano-filaments widely used as superhydrophobic materials. Nanostructure design with nano-filaments of pSi-SH coating (Figure 11) exhibits a water contact angle (CA) of 97° . After surface modification with perfluoropolyether (HD 1101Z), the coatings (f-pSi-SH) become nearly perfect anti-wetting with a higher water contact angle of 177.7° [28]). They also reported, the pSi-V coatings with vinyl terminated surface modification also showed higher water contact angle than pSi-CH_3 (methyl terminated or pSi-Ph (phenyl terminated) mainly due to nano structure formation on the surface.

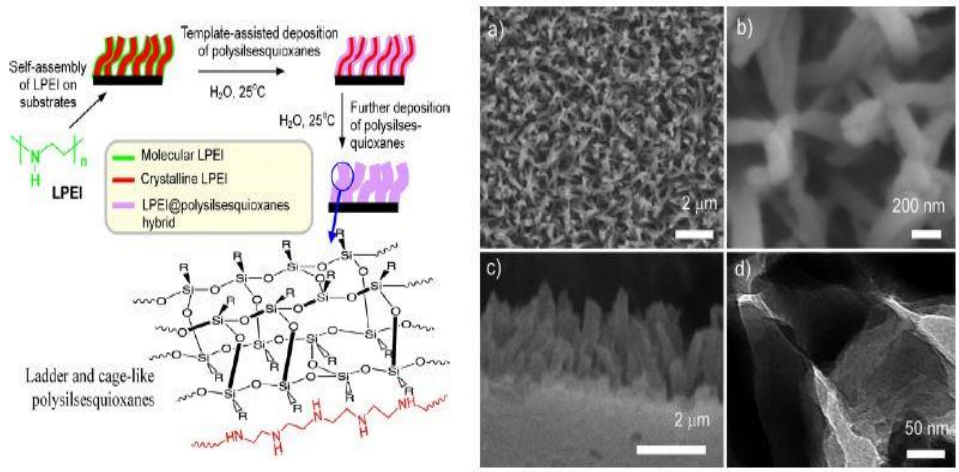

Figure 11. Schematic Representation of the Formation of nanofilament Coating of LPEI@polysilsesquioxanes (left). And SEM (a–c) and TEM (d) images of LPEI@pSi–SH nanofilament coating on a glass substrate. (Reprinted from ref [28])

2.3 Mechanism of micro–nano structure formation

Micro–nano structure formation on the treated cotton fabric played an important role of changing surface energy, surface roughness resulting surface superhydrophobicity. Mechanism of formation micro–nano structure can be discussed in three steps–

Step 1: ODA molecules in aqueous dispersion, ODA known as stearylamine having monoalkylamines compounds that contains a primary aliphatic amine group. ODA practically insoluble in water and

strong basic compound due to its pKa. When ODA pour into water in a glass bottle ODA powder floated on the water and make separate layer. But when heated above its melting temperature and ultra-sonication with water, ODA molecules dispersed in water by magnetic stirrer.

Step 2: Self-assembled ODA layer, when adding acetic acid into dispersed ODA solution, amine group start to protonation and formed unstable hydrogen bonds themselves or with water through hydroxyl group due to van der Waals dispersion forces and dipole-dipole interactions. Thus, ODA self-assembled monolayer is formed in aqueous solution.

Step 3: Aggregation of ODA/HDTMS, in aqueous solution, organosilanes can hydrolysis and oxide network are formed in solution to produces a mixture of cages, ladder like, petal and network structures through HDTMS hydrolysis or poly condensation reactions (as scheme 2.b). When HDTMS added into the ODA solution, hydroxyl network bind with ODA monolayer and formed petal like structure in the solution. During dip coating by immersing cotton fabric, aggregated ODA/HDTMS coated with substrate through Si-O-Si bonding by hydrolysis or polycondensation reaction. And amino functional silanes like chemical structure is formed.

In this study, Cotton fabric was treated with ODA/ HDTMS by dip coating methods. The coating material preparation and coating

treatment methods are illustrated in details as scheme 1 (a). Coating preparation of ODA/HDTMS mixer by magnetic stirrer last for an hour. After prepare coating solution cleaned cotton fabric dip into the ODA/HDTMS coating solution for 15min then dry at 100℃ temperature for 1hour by oven. The preparation mechanism of micro-nano formation methods of ODA/HDTMS coating solution is illustrated by scheme 1(b). And the chemical structure of ODA, HDTMS and possible chemical structure of aggregated ODA/HDTMS on cotton is illustrated by scheme 2 a, b and c respectively. The effect of surface roughness by ODA/HDTMS coating treatments on superhydrophobicity (WCA, WSA), and self-healing performance are explained in result and discussion section. Also the effect of aggregation of ODA/HDTMS coating solution on breathability by the pore determination. And the influence of ODA/HDTMS aggregation behavior on surface roughness and surface energy by adjustments ODA or HDTMS also discussed in result and discussion section.

2.4 Challenges of superhydrophobic surface

As already discussed, most approach to design superhydrophobic surfaces are mainly based on fabricating micro–nano structure by combination of low surface energy materials and nano particles. But, they have non–covalent bond properties so it can remove easily from fabric surface by external force. Because of unique properties of ZnO, TiO_2, SiO_2, and $Al2O_3$ nanomaterials widely used in superhydrophobic surface and other purposes.

Despite of some of the potential benefits, nanoparticles has possible adverse effects on human and environments. Recent few research revealed, nano materials can easily enter human body through skin or lung via respiratory and lead to toxicity such as DNA damage, protein misfolding, membrane damage, production of reactive oxygen species etc. [45,46,47]. Below Graphical picture depicted how nanoparticles makes in different production level, how nanoparticles mixed with environments and how nanoparticles get entry in human body through different routes (figure 12). Due to its diverse effect on human body, environment and ecology, nano–materials are considered as toxic materials and harmfulness. Recent years various approach has been introduced to fabricate superhydrophobic surface excluding both nanoparticles and toxic materials such as fluorine free, solvent free, waterborne solution system etc. Such steps may help to lead green surface modification to design superhydrophobic surface and inspired to large scale production.

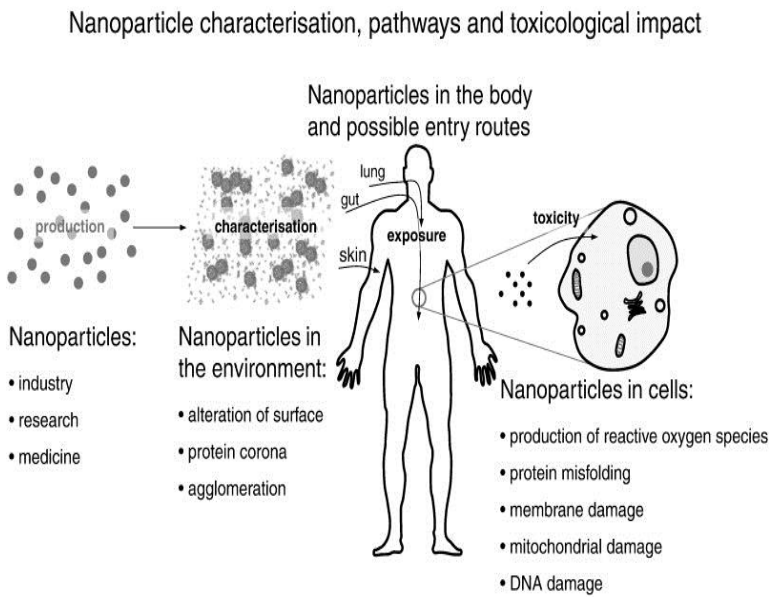

Figure 12. Illustration of how nanoparticles can get access to the body mainly via the airways, the skin or via ingestion (Reprinted from ref [45]).

Fluoro-containing substance that are used for lowering surface energy materials also impact on ecology and its harmful for human health. long-chain PFCs can bio-accumulate as they move though food webs. Compound with long perfluoroalkyl chain length (8 or more) are generally more bio-accumulative than those with 7 or less. Because of these characteristics PFCs has an environment impact. Research on animal found that perfluorooctane sulfonate, (PFOS) and perfluorooctanoic acid (PFOA) has potential impacts [48].

Durability of superhydrophobicity, Cost and clothing comfort also challenging issues for superhydrophobic surface.

Chapter 2. Experimental

1. Materials

1.1 Substrate:

In this study, 100% cotton bleached, un-mercerized woven fabric was used as substrate, purchased from Testfabrics, Inc (Korea). The detailed information is summarized in Table 1.

Table 1. Characteristics of Cotton fabric

Fiber content	100% cotton fabric
Weight (g/m^2)	120
Weave type	Plain weave
Thickness(mm)	0.22
Weave density (in inch)	133X72
Test method	AATCC TM 133

1.2 Materials:

Octadecylamine, ODA (90%), linear formula $CH_3(CH_2)_{17}NH_2$), molecular weight 269.51 g/mol, were obtained from Aldrich Chemical Co. (USA). Hexadecyltrimethoxysilane, HDTMS (85%), molecular weight 346.62 g/mol, linear formula $H_3C(CH_2)_{15}Si(OCH_3)_3$ were also purchased from Aldrich Chemical Co. (USA). Distilled water used as solvents. Acetic acid solution was purchased from SAMCHUN (Korea). For measuring water vapor transport (WVTR) and moisture permeability Showa (Japan) calcium chloride, glanular (first class) was purchased and used. It is note that, all reagents were used without further purification.

Chemical structure of ODA and HDTMS:

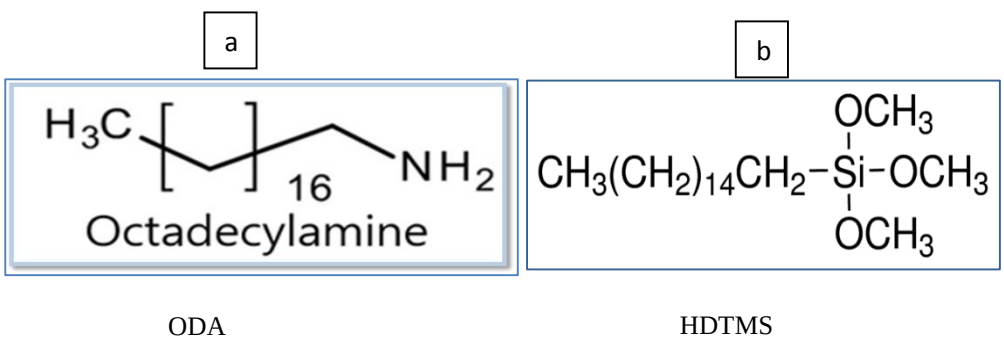

Figure 13. Chemical structure of (a) ODA and (b) HDTMS

2. Coating

2.1 Preparation of coating solution and coating treatment

0.5g ODA dissolved in 50g distilled water by ultrasonication at 60°C for 15 min then magnetic stirrer 1hr till dissolved well with adding few drops of acetic acid. Then added HDTMS in the solution with different molar ratio (for example ODA/HDTMS 1:1 molar ratio 0.64g HDTMS added) and stirrer more 1hr at same temp. 60°C till mix them well. The final milk white solution was ready for coating solution.

A dip coating method was applied for coating solution onto cotton fabric. A piece of 9 X 9 cm 100% cotton fabric sink into the solution as dip coating for 15 min at 60°C. And finally dry the coated sample at 100°C for 1hr by oven to get superhydrophobic cotton fabric (as shown in scheme 1) It is note that, dip coating treatments were followed by the same methods for different molar ratio such as ODA/HDTMS 3:1/2:1/1:1/1:2/1:3 respectively with same conditions. Total amount of coating materials calculated in grams according to molar ratios such as 1: 2 (mol mol^{-1}) means 3 moles ODA/HDTMS coating materials treated by cotton substrate. After coating treatment followed by drying no apparent change of the fabric color. The molar ratio of ODA/HDTMS in the solution expressed by treatment code as UT, OH_31, OH_21, OH_11, OH_12 and OH_13 represents untreated cotton ODA/HDTMS 3:1/2:1/1:1/1:2/1:3 respectively. For example, OH_31 represents coating of ODA and HDTMS as 3:1 molar ratio.

Also, OH_20, OH_30 and OH_02, OH_03 are represents coating of only ODA 2 mol, 3 mol and coating of only HDTMS 2 mol, 3 mol respectively (as table 2).

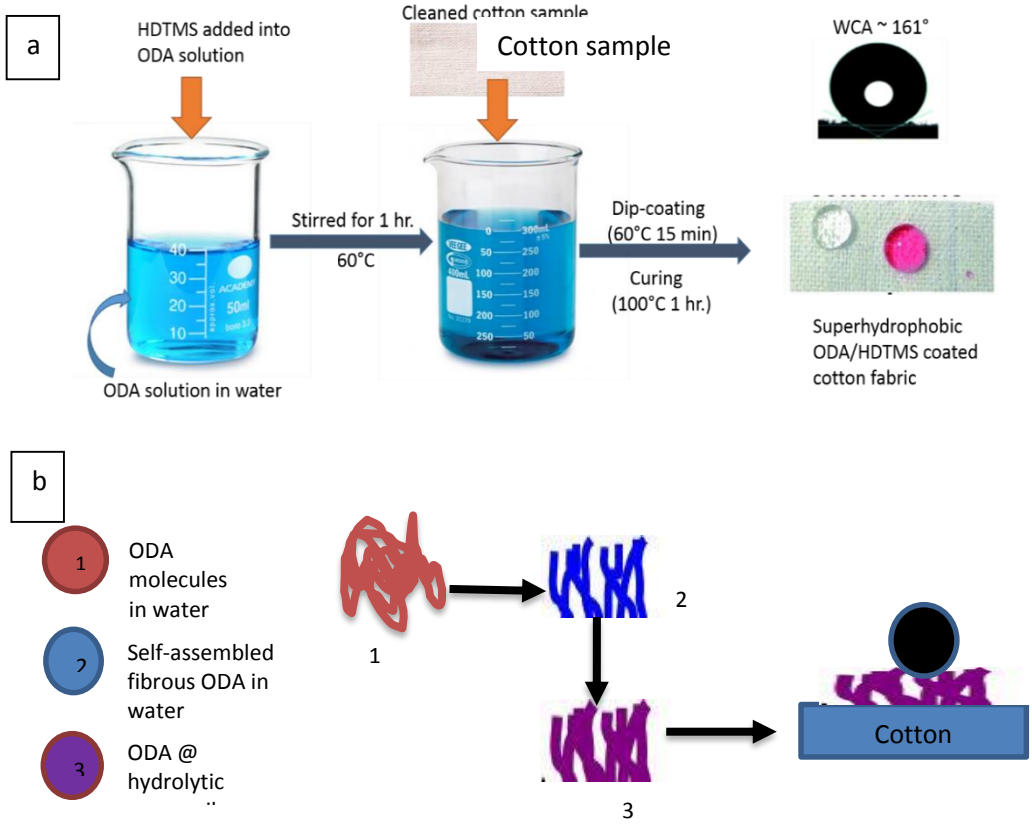

Scheme 1. Preparation method of coating solution, coating treatment (a) and mechanism of nano-filament formation (b)

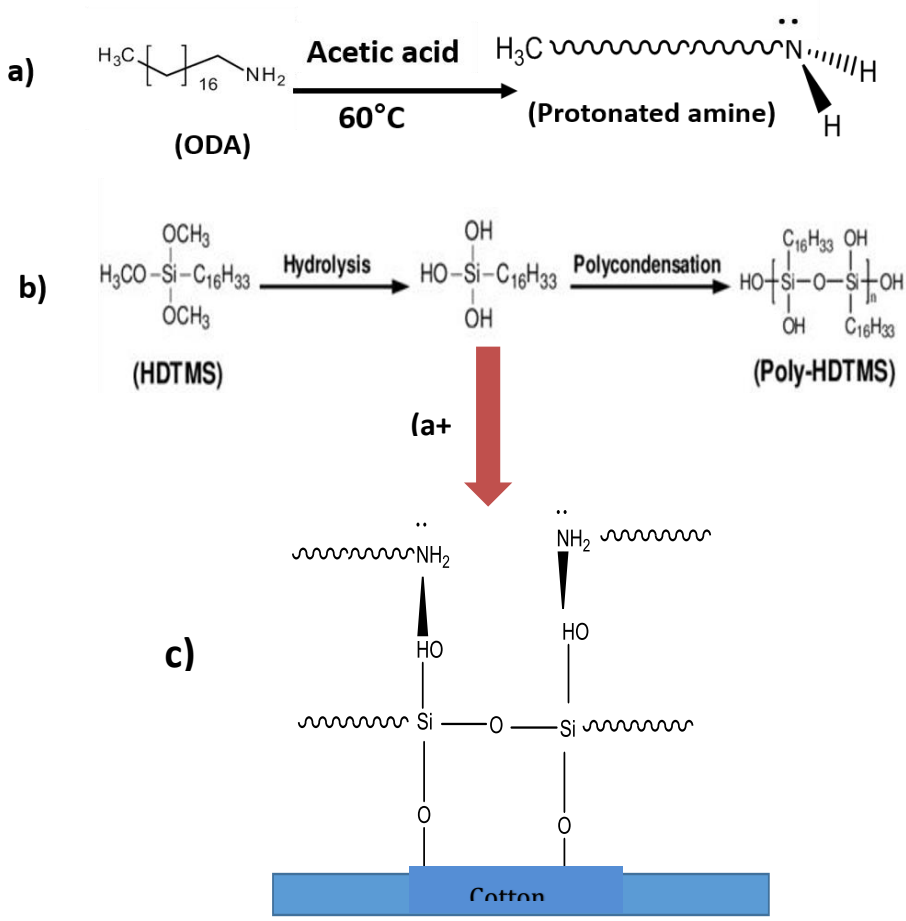

Scheme 2. chemical structure of (a) ODA and (b) HDTMS and (c) proposed chemical structure of coating materials

Table 2. Specimen code and description of the experimental condition

Treatment codes	Descriptions
UT	Untreated
OH_31	Specimen coated with ODA/HDTMS 3:1 molar ratio
OH_21	Specimen coated with ODA/HDTMS 2:1 molar ratio
OH_11	Specimen coated with ODA/HDTMS 1:1 molar ratio
OH_12	Specimen coated with ODA/HDTMS 1:2 molar ratio
OH_13	Specimen coated with ODA/HDTMS 1:3 molar ratio
OH_20	Specimen coated with 2 mol ODA only
OH_30	Specimen coated with 3 mol ODA only
OH_02	Specimen coated with 2 mol HDTMS only
OH_03	Specimen coated with HD 3 mol HDTMS only

3. Characterization

3.1. Observation of surface morphology (FE-SEM)

The surface morphology of the sample was measured by a field emission scanning electron microscope; FE-SEM, AURIGA, Carl Zeiss, Germany). To prevent the charge-up phenomenon that electrons accumulate on the sample surface before measurement, a sputter coater (EMACE 200, Leica microsystems, Austria) under argon gas at a current of 30 mA, a pressure of 0.05 mbar, Platinum coating (thickness: about 15 nm) was performed for 200 seconds at a distance of 50 mm between samples.

3.2 Functional group analysis (FT-IR spectra)

To identify different functional group on the treated fabric surface by Fourier Transform Infrared Spectroscopy (FT-IR; Nicolet iS50, Thermo Fisher Scientific, USA). The treated cotton sample fabric surface was analyzed in absorbance mode in the range of 350-7800 cm^{-1}.

3.3 The chemical composition analysis (XPS spectra)

The chemical composition of the cotton fabrics before and after ODA/HDTMS coating treatment was examined by X-Ray Photoelectron Spectroscopy (XPS; (AXIS-his, Kratos Inc., USA). The Chemical composition change graphs of XPS wide scan survey and component percentages in the C1s spectra and the atomic

concentration of C and O measured for cotton fabric before and after ODA/HDTMS treatments.

3.4 Evaluation of Superhydrophobicity

3.4.1 Static contact angle

The static contact angle was measured using a contact angle meter (Theta lite optical tensiometer, KSV Instruments, Finland). Cut the sample to be measured using a scotch tape to place on an edge of the slide glass and lay flat Respectively. And 3 samples each having a size of 5 cm × 10 cm were prepared for each condition. Distilled water was dropped (drops size 3.5±0.5 [μm]) of on the vertical direction to measure the contact angle. The static contact angle values for the sample reported were the average of five measurements.

3.4.2 Shedding angle

Water shedding angle (WSA) of various samples was measured by the method of Zimmermann et al. [49] after releasing a drop of water (12±0.5 μl) in a height of 1cm, the minimum angle of inclination at which the drop completely rolls off the surface was determined. According to Zimmermann theory water drops from 1 cm and drops must be roll off 2 cm or more at minimum angle inclination. The

shedding angle values for the sample reported were the average of five measurements with change of 0.5° inclination angle.

3.5. Durability test

3.5.1 Washing durability

In order to evaluate the washing durability of the sample subjected to the superhydrophobic treatment, measure contact angle after repeated washing with standard course using Tromm® (LG) drum washing machine. At the time of washing, fillet case is dumped to 25% of laundry load and about total 12 pieces of pillow case. Five samples were prepared and placed in a pillow case sample of size 9x9 cm was cut from the edge of the fillet case in the width and width direction. And each was stuck at a distance of 1.5 cm. The standard course was laundered – rinse (twice) – dehydrated for a total of 59 minutes. Washing was carried out without putting detergent in cold water. After washing the sample was dried at room temperature and measured contact angle and compare.

3.5.2 Tape and peel test

To evaluate adhesive strength of the coating sample, a (Scotch-Brite, 3M) tape was used multiple times on the superhydrophobic coated surface. It is note that, adhesive tape peeling test was employed manually and moderate pressure was used by hand to use Scotch-

Brite, 3M tape with handle on the fabric surface. To evaluate change of the superhydrophobicity by measuring water contact angle with multiple peeling. For example, each sample peeled 10 times once and measure water contact angle and roll-off angle. To verify adhesive strength, we peeled up to 50 times and compare respectively.

3.6 Self- healing test

3.6.1 acid/alkali test

Two methods were employed to evaluate self-healing properties of the coated superhydrophobic fabric by acid and alkali test. To examine self-healing properties coated fabric, pH 1-11 chemical solution were prepared by adding hydrochloric acid, HCl (pH 1-7) and sodium hydroxide, NaOH (7-14) to distilled water. To conduct acid/alkali pH test 150 ml solution were prepared pour into a glass dish where treated fabrics were attached by polytetrafluoroethylene (PTFE) tape at bottom of the glass dish. The treated fabric soaked into pH solution for 15 min then rinsed by tap water and dry at room temperature and measure WCA. Then the chemical damaged fabric heated at 100° C for 15 min or 24 hours dry at room temperature then checked WCA and compared.

3.7 Breathability evaluation

3.7.1 Air permeability

To measure and compare air permeability ASTM, American Society for Testing and Materials test method D737−04 (2016) [50], an air permeability testing device (FX 3300, TEXTEST, Switzerland) was used to measure and compare the air permeability. Considering that the measuring head area of the test apparatus is 38.3 cm^2. Three samples each having a size of 20 cm x 20 cm were prepared, and a total of five samples were prepared under a pressure of 125 Pa. The measurements were averaged and expressed in units of cubic feet per minute (CFM). Before the measurement, the sample was conditioned at a temperature of 21 ± 2 ° C and a relative humidity of 65 ± 5%.

3.7.2 Water vapor transport rate (WVTR)

The moisture permeability is measured according to the calcium chloride method of KS K 0594 (2015) [51] respectively. Before the experiment, the moisture−permeable cup was prepared by pre−heating to 40 ° C. Three test pieces each having a diameter of about 70 mm were prepared. In the permeable cup (as figure 14.) 33 g of calcium chloride was filled and the surface was flattened using a spoon. Raise the specimen to maintain the spacing of 3 mm between the calcium chloride and the packing and ring. And then fixed with a

butterfly nut. The prepared specimen is placed in a constant-temperature and humidity chamber at a temperature of 40 ± 2° C and relative humidity of 90 ± 5%. After one hour, the test piece was taken out and the mass a_1 was immediately measured. After measured weight then put again in the machine and wait for 1 hour and taken out to measure mass a_2 immediately.

$$p = \frac{a_2 - a_1}{S} x\ 24 \qquad (5)$$

Where,

P: Water permeability (g / m^2. 24h)

$a_2 - a_1$: Mass change of the specimen after 1 hour (g / h)

S: Permeable area (m^2)

The water vapor permeability was calculated using equation (5), and the measured values were averaged three times. In this study, the moisture permeation area S was 6 cm that is changed to 0.002826m^2 from the diameter of 6cm of exposed test specimen. Multiplying 24, the water vapor permeability per unit area for 24 hours as 1 day to be displayed as a standard unit expression as g/m^2x24 hr. (gram per square meter a day)

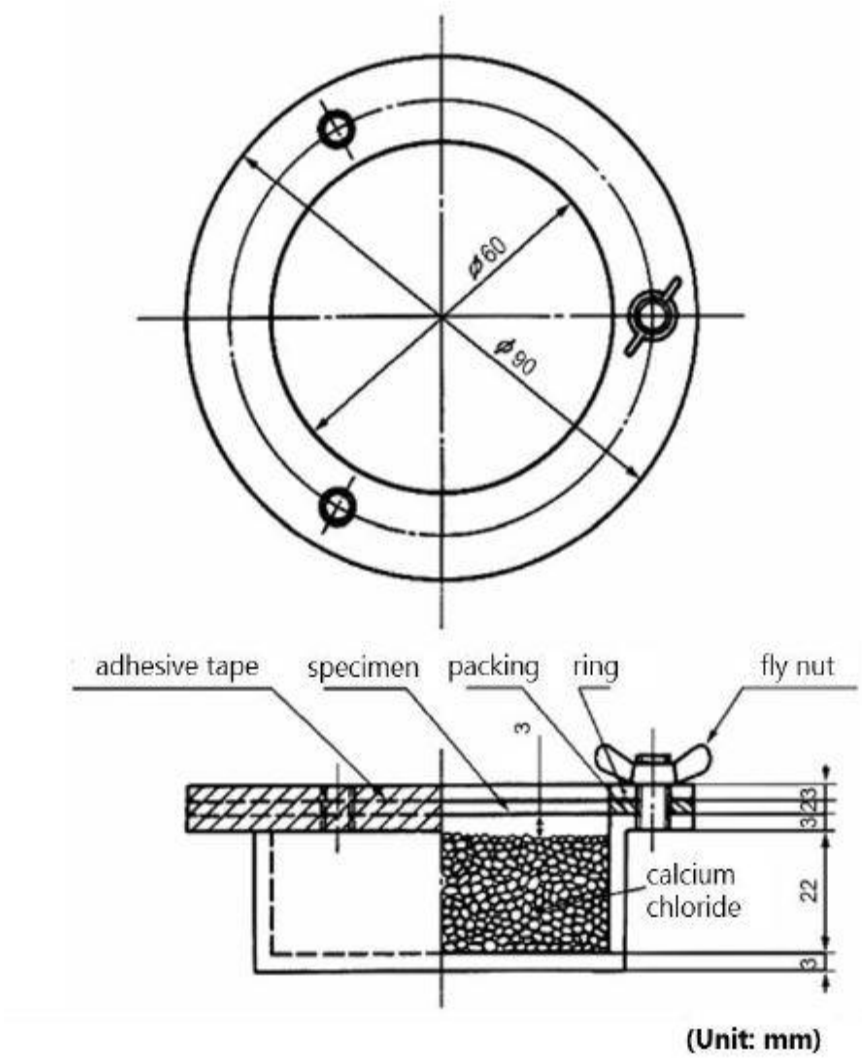

Figure 14. Schematic diagram of water vapor transport, WVTR measurement equipment via calcium chloride method [51].

Chapter 3. Results and discussion

1. Surface morphology according to molar ratios

1.1 Surface morphology of the fabric treated with ODA solution alone

When sample was treated by ODA alone with different concentration, the difference in the surface morphology of the treated sample was observed, as shown in Fig.15. Depending on the concentration of ODA solution, the monolayer formation on the coated fiber surface analyzed by FE-SEM images in different scale magnifications. Here we reported FE-SEM image with 1000 and 5000 times of magnification to observed surface morphology on the treated fiber surface. When sample was treated with 2 mol ODA solution, smooth surface morphology appeared as untreated surface. When ODA concentration was increased to 3 mol surface morphology still remain unchanged but few particles are observed on the fiber surface. Since ODA is amphiphilic in nature so even through with increasing of ODA in to the coating solution slight roughness in showed as monolayer on the coated surface.

Specimen	Magnification	
	X1000 (10μm)	X 5000 (2μm)
OH_20	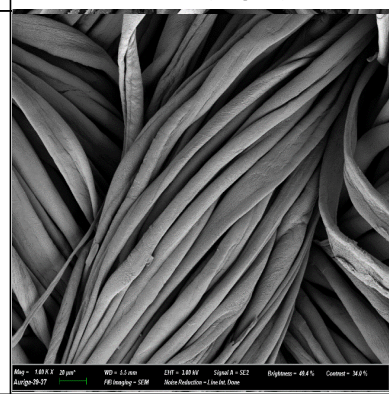	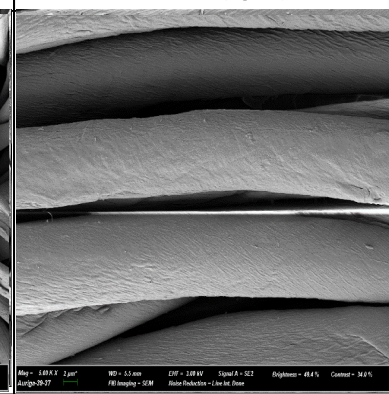
OH_30	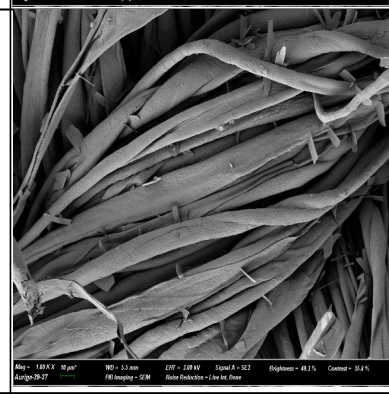	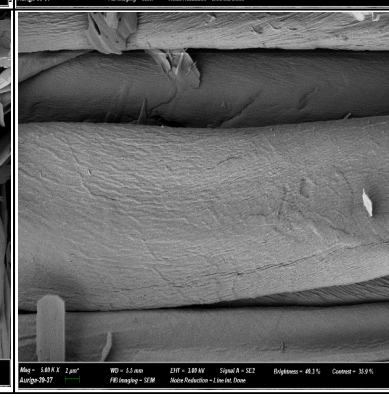

Figure 15. SEM images illustrated the change in surface morphology of only ODA solution coated cotton fabrics.

1.2 Surface morphology of the fabric treated with HDTMS solution alone

Similarly, when sample was treated by HDTMS alone with different concentration, the difference in the surface morphology of the treated sample was observed, as shown in Fig.16. Depending on the concentration of HDTMS solution, the hydrolytic alkyl silanes crystal on the coated fiber surface analyzed by FE-SEM images in different scale magnifications. Here we reported FE-SEM image with 1000 and 5000 times of magnification to observed surface morphology on the treated fiber surface. It is noted that, long chain HDTMS not only used as hydrophobic agents and also acts as lowering surface free energy but also act as a bonding to the fabric that support to aggregate particles by polymerization. But when HDTMS treated alone with various concentration no significant nanostructure is found. When sample treated by 1 mol HDTMS apparently no changes of surface morphology compared with untreated sample, but when concentration increased to 2 mol and 3 mole surface became more rough.

Specimen	Magnification	
	X1000 (10μm)	X 5000 (2μm)
OH_02	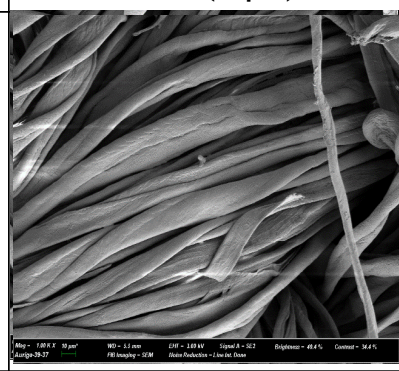	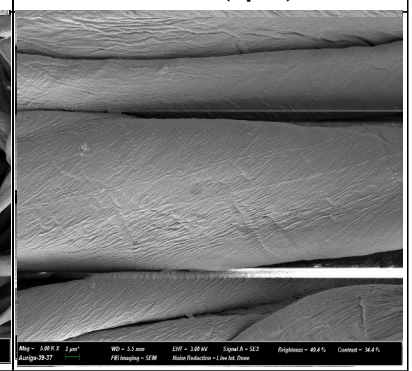
OH_03	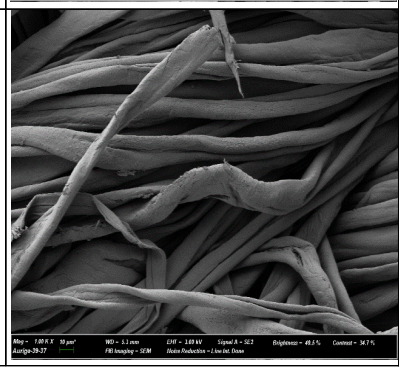	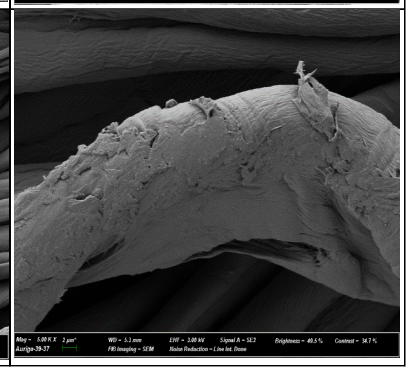

Figure 16. SEM images illustrated the change in surface morphology of only HDTMS solution coated cotton fabrics.

1.3 Surface morphology of the fabric treated with ODA/HDTMS solution

To evaluate surface morphology of ODA/HDTMS coated fabric FE-SEM images were analyzed in different resolution as X1000 in 10μm and X5000 in 2 μm scale. As figure 17 and 18 depicted SEM image of cotton fabric before and after ODA/HDTMS coating treatments. ODA/HDTMS molar ratio in the coating solution effects the surface morphology. As figure 17 Sample UT (untreated) cotton fabric showed very smooth fiber surface and apparently no surface roughness thus fabric absorbed water right after drops on the surface due to cellulosic unit (OH abundance). ODA is hydrophilic in nature and HDTMS used as hydrophobic agents by reducing surface free energy, so when HDTMS increased into ODA/HDTMS coating solution significant changes of surface morphology was shown as figure 17 and 18. As scheme 2 when ODA and HDTMS aggregate together surface became micro-nano roughness. For example, when cotton fabric treated with ODA/HDTMS 3:1 molar ratio (as sample OH_31) hydrolytic organosilanes aggregated with self-assembled ODA layer thus formed nano structure on the coated surface. As already mentioned, HDTMS act as hydrophobic to the fabric that support to aggregate by polymerization so that when HDTMS increased to coating solution surface roughness increased shown in SEM images. According to scheme 2 when HDTMS increased into the

ODA/HDTMS solution thus increased aggregation and provides more roughness on fiber surface. The best condition reported on ODA/HDTMS 1:2 molar ratio indicates highest surface roughness. According to Cassie–Baxter law when surface energy became low and micro and structure are formed surface became hydrophobic [35]. And due to air pockets water easily drag–off from fabric surface results self–cleaning fabric is demonstrated. We also reported excess HDTMS decreased surface roughness as OH_13 due to abundance HDTMS disturbs aggregation of ODA/HDTMS and fills inter particles gaps thus reduce nano structure as figure 17. Similar results also reported by Wang et.al. [52].

Specimen	Magnification	
	X1000 (10μm)	X 5000 (2μm)
UT	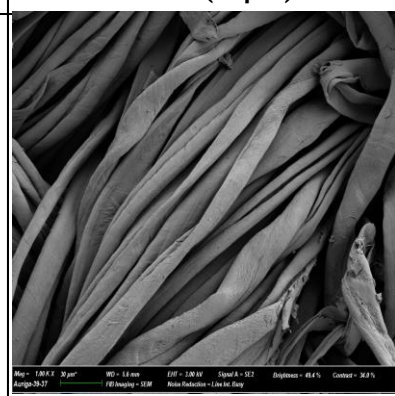	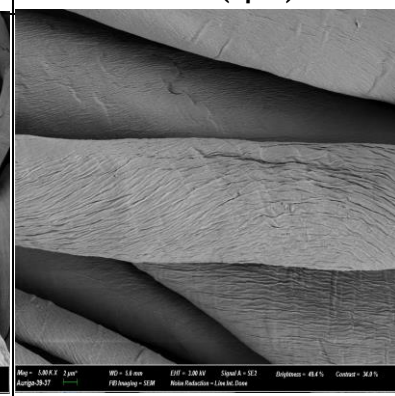
OH_31	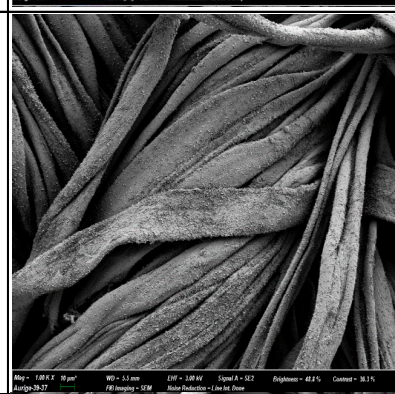	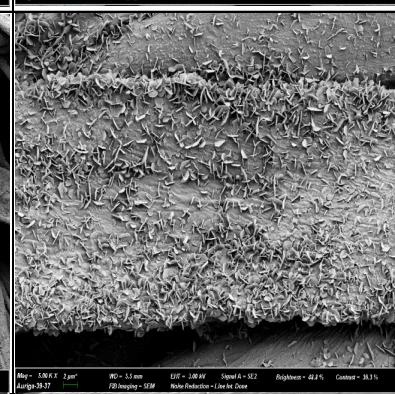
OH_21	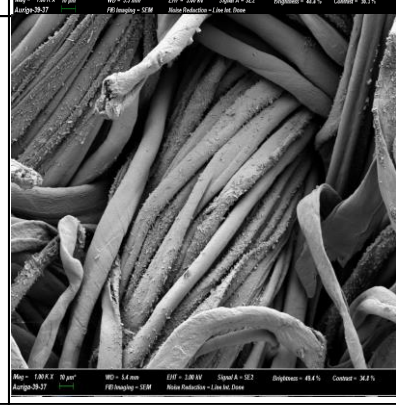	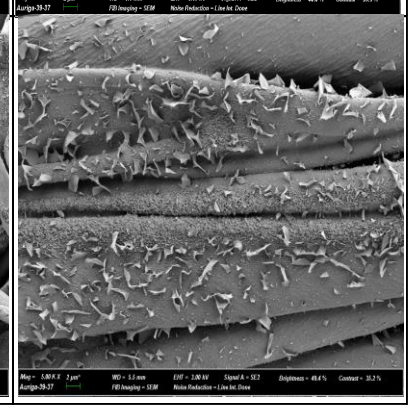

Figure 17. SEM images illustrated the change in surface morphology of ODA/HDTMS solution coated cotton fabrics with different molar ratios (continued).

Specimen	Magnification	
	X1000 (10μm)	X 5000 (2μm)
OH_11	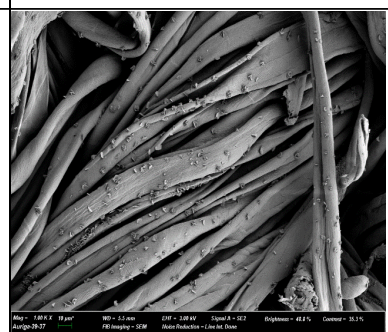	
OH_12	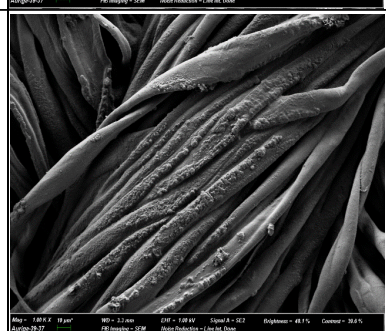	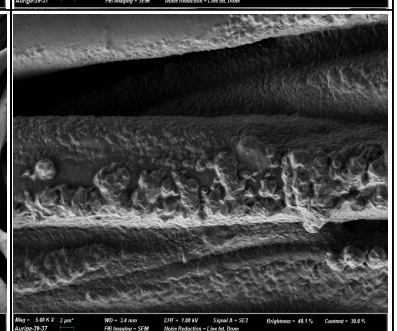
OH_13		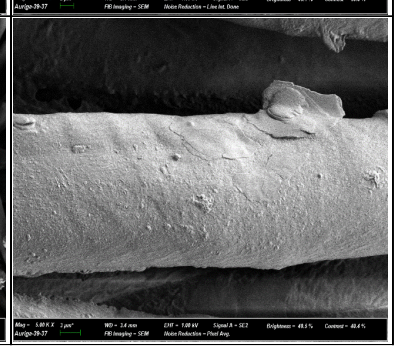

Figure 18. SEM images illustrated the change in surface morphology of ODA/HDTMS solution coated cotton fabrics with different molar ratios.

2. Changes of surface properties due to ODA/HDTMS treatment

2.1 Functional group

The functional groups of the cotton fabric before and after ODA/HDTMS coating treatment was examined by FT-IR. After ODA/HDTMS coating new peaks appeared on 2916 cm^{-1}, 2850 cm^{-1}, weak peaks at 1560 cm^{-1} and peaks at 1029 cm^{-1} confirmed that C-H_2/CH_3, long alkyl chain amine functional group (NH), and Si-O-Si strong covalent bond appeared in FT-IR spectra respectively. From other research 2855 cm^{-1} and 2929 cm^{-1} was assigned to the -CH/-CH_2- stretching and CH_3- stretching of HDTMS [53,54]. The region of 1028 cm-1 was attributed to the asymmetric stretching vibration of Si-O-Si bonds [55].

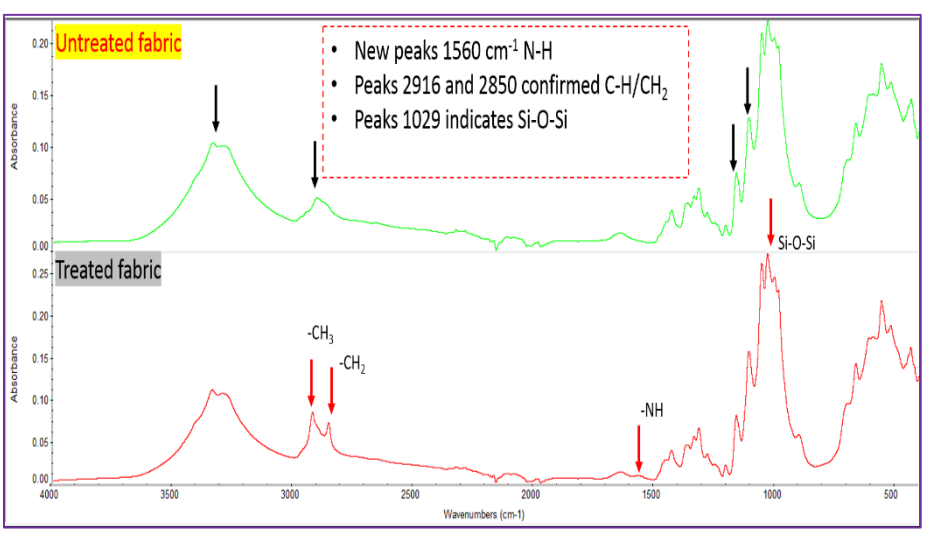

Figure 19. FT-IR analysis of uncoated cotton and ODA/HDTMS coated cotton fabric

2.2 The chemical composition

The chemical composition of the cotton fabric before and after ODA/HDTMS coating treatment was examined by XPS wide scan survey and C1s XPS fitting curve. The untreated cotton showed only C1s and O1s peaks in XPS wide scan survey. But after ODA/HDTMS coating treatments the presence of new peaks N1s at 400 eV, Si 2p and Si 2s at 105 eV and 155 eV confirmed ODA/HDTMS successfully coated on the fiber surface as figure 20 (a). C1s fitting curve was evaluated to be confirmed that ODA/ HDTMS aggregated and well coated on the fiber surface by the changes of C1s curve and change of C−C/C−H and O−C−O binding energy and introducing of C−Si and C−N binding is forms as figure 19(b) & (c). The high resolution of C1s peak exhibits three distinct peaks C−C/C−H peak at 284.44 eV, C−O peak at 286.13 eV and O−C−O peaks at 287.68 eV for untreated cotton fabric. After ODA/HDTMS coating treatments the peaks of C−N at 286.57 eV and C−Si bonds peak at 283.91 eV can be fitted from XPS spectra. The changes of XPS wide scan survey as 20 (a) and C1s changes fitting curve from untreated cotton to ODA/HDTMS coated treated fitted curve as 20 (b,c) indicates ODA/HDTMS successfully coated on the cotton fiber surface. Thus, changes superhydrophilic surface to superhydrophobic cotton surface.

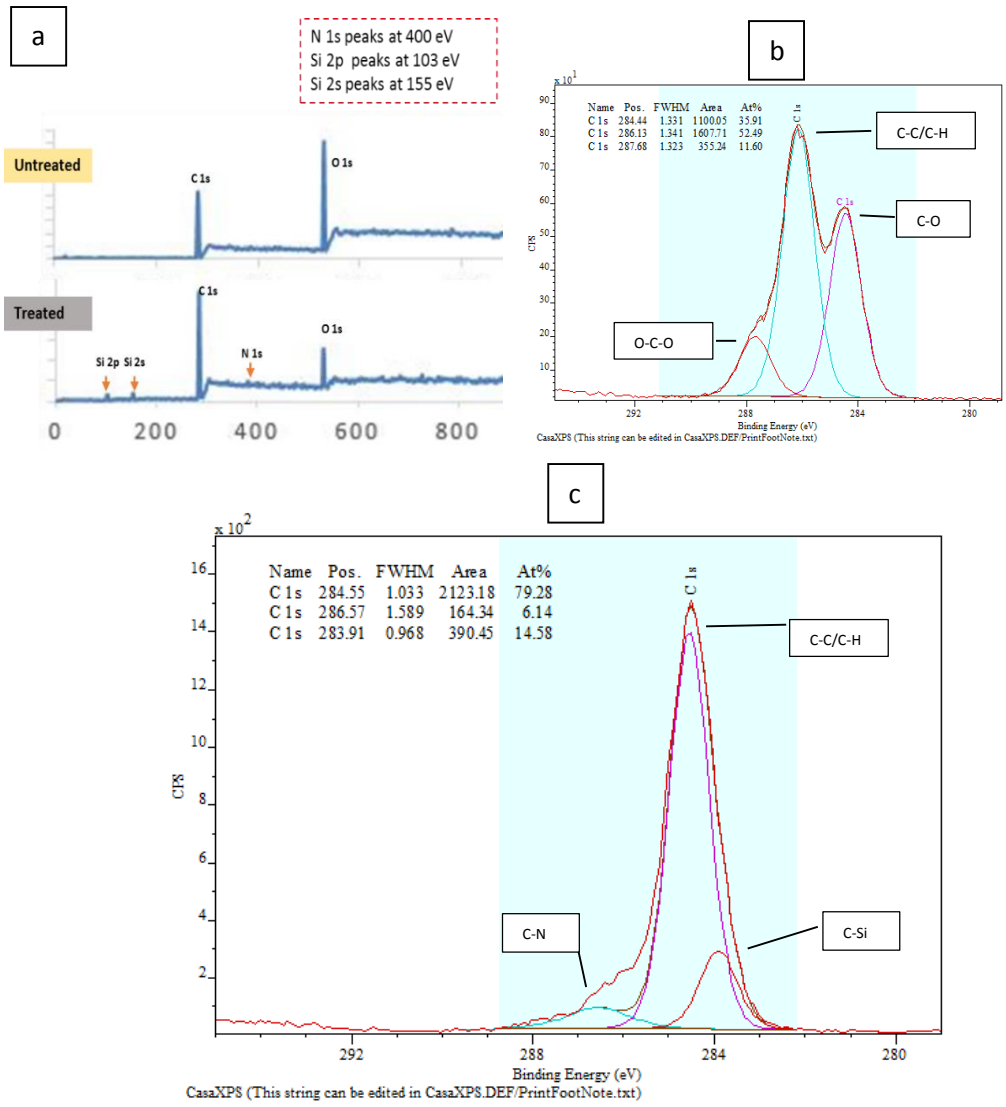

Figure 20. (a) XPS survey spectra of the cotton fabric before and after treatments; C1s XPS spectra with fitting curves of (b) untreated cotton, (c) ODA/HDTMS coated cotton fabric.

3. Surface wettability according to molar ratios

1.1 Static contact angle

Anti-wetting properties of ODA/HDTMS treated fabric was measured by static contact and shedding angle. As compared treated fabric with untreated cotton fabric. When 100% cotton (untreated fabric CA=0º) was treated by only ODA and DHTMS coating, water contact angle WCA showed 0 º and 148º respectively. The tendency of increasing superhydrophobicity depends on the molar ratios of ODA/HDTMS. ODA is amphiphilic in nature thus showed hydrophilic properties character in aqueous dispersion due to its chain migration characteristics with selective solvents. So ODA coated fabric remained hydrophilic but due to HDTMS hydrophobic in nature when untreated cotton fabric coated with HDTMS solution fabric showed hydrophilic and highest WCA recorded 148º. When untreated cotton fabric was coated ODA/HDTMS, fabric became superhydrophobic. It was also noted that, ODA/HDTMS molar ratio in the coating solution affected the hydrophobicity of the coated fabrics. also when HDTMS increased into the coating solution surface roughness increased and decreased surface free energy. Thus dramatically changed static contact and shedding angle due to its micro nano roughness and surface free energy. So when HDTMS increased water contact angle was increased and shedding angle decreased. As figure 21 shows the effect of ODA/HDTMS according to molar ratios on WCA of the

treated fabrics. When ODA/HDTMS molar ratio was 3: 1, the WCA was below 150º. When the molar ratio was changed to 2: 1 the CA increased to 153.7º. In this study, best water repellency was found at 1:2 molar ratios as highest WCA 161.4º by the solution of ODA/HDTMS of 1: 2. However, when the DA/HDTMS ratio was 1: 3 water repellency was decreased due to excess HDTMS fills inter particle gaps thus changes of water contact angle to 154º.

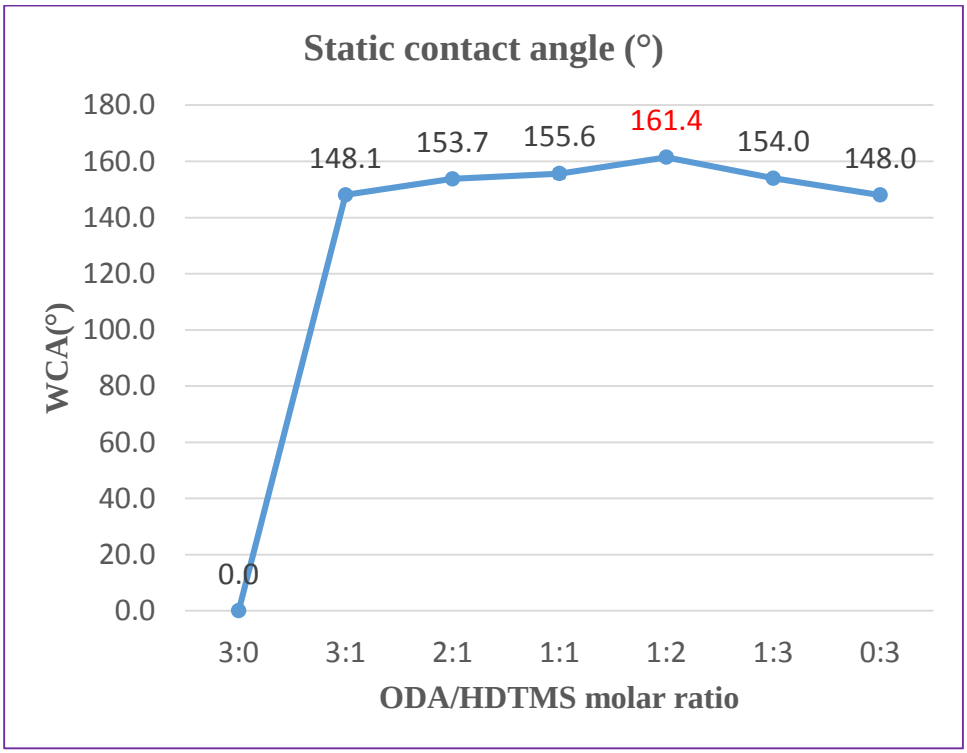

Figure 21. Static contact angle of water on ODA/HDTMS treated cotton fabric under various molar ratios.

1.2 Shedding angle

Similarly, shedding angle was measured to evaluate superhydrophobic properties of ODA/HDTMS coated fabric. As mentioned ODA is hydrophilic in nature and after treated by only ODA shedding also not measurable. Because water drops absorbed by ODA treated fabric right after drops on the surface. But when cotton fabric treated with HDTMS fabric surface showed shedding angle 17° due to HDTMS treated fabric increased micro–nano roughness on the surface compared to untreated fabric. ODA/HDTMS molar ratio similarly effect on shedding angle. As figure 22 shows the effect of ODA/HDTMS molar ratio on WSA of the treated fabrics. When ODA/HDTMS molar ratio was 3: 1, the WSA was 12° . When the molar ratio was changed to 2: 1 the CA decreased to 10° . In this study, best shedding angle was found at 1:2 molar ratios as highest WSA 8.5° by the solution of ODA/HDTMS of 1: 2. This is possibly because at 1:2 ODA/HDTMS molar ratios formed highest surface roughness and lowest surface free energy from HDTMS thus changed Wenzel state to Cassie Baxter state. When ODA/HDTMS molar ratio was further increased to 1:3 shedding angle increased to 12º due to excess HDTMS into the solution it disturbs ODA/HDTMS aggregation thus effect of making nano structure.

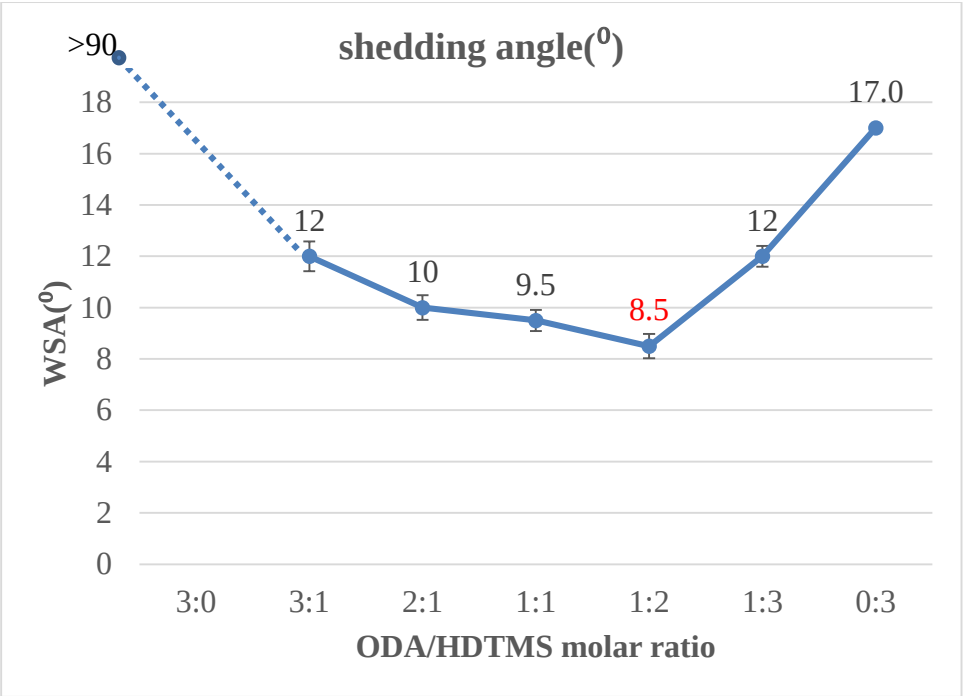

Figure 22. Shedding angle of ODA/HDTMS treated cotton fabric under different molar ratios

4. Changes of functionality due to ODA/HDTMS treatment

4.1 Durable functionality of ODA/HDTMS treated fabric

4.1.1 Laundry washing durability

Durability of superhydrophobic coated materials is important requirements for long time use or demand for practical application. To evaluate washing durability of ODA/HDTMS treated superhydrophobic cotton were examined by LG drum laundry

washing machine at 25% loading. After 1 laundry washing cycle fabric maintained water contact angle above 150º (WCA=151.5º) but water shedding angle was decreased significantly as WSA 14º. After repeated washing as 5 washing water contact angle was decreased not significantly and it was maintained WCA as 142º but water shedding angle was changed dramatically. After 5 laundry washing cycle water shedding angle showed 17º as figure 23. To find out the reason for increasing/decreasing of WCA/WSA is that, during laundry washing water induced hydrophilic group on to the surface and due to friction between fabric and drum of the washing machine nano clusters were removed thus changing wettability. Yang et.al. reported that during washing water induces hydrophilic polar groups that react with coating materials it causes surface molecular rearrangement and a decrease in the static contact angle [56].

Interestingly, partial damage of ODA/HDTMS coating layer by washing treatment surface changed wettability but when sample dried 24 hrs. at room temperature nearly restored its superhydrophobicity. This is because of the rotation and movement of the ODA/HDTMS chains by thermodynamically driven that gives mobilized energy thus minimizing the surface tension [52,58]. The tendency of repeated restoring properties became slow and difficult from after 5 repeated cycle thus healing time required more than 48hrs. This is possibly because functional groups addition by water

through washing and loss of particle remove by friction between drums and fabric surface.

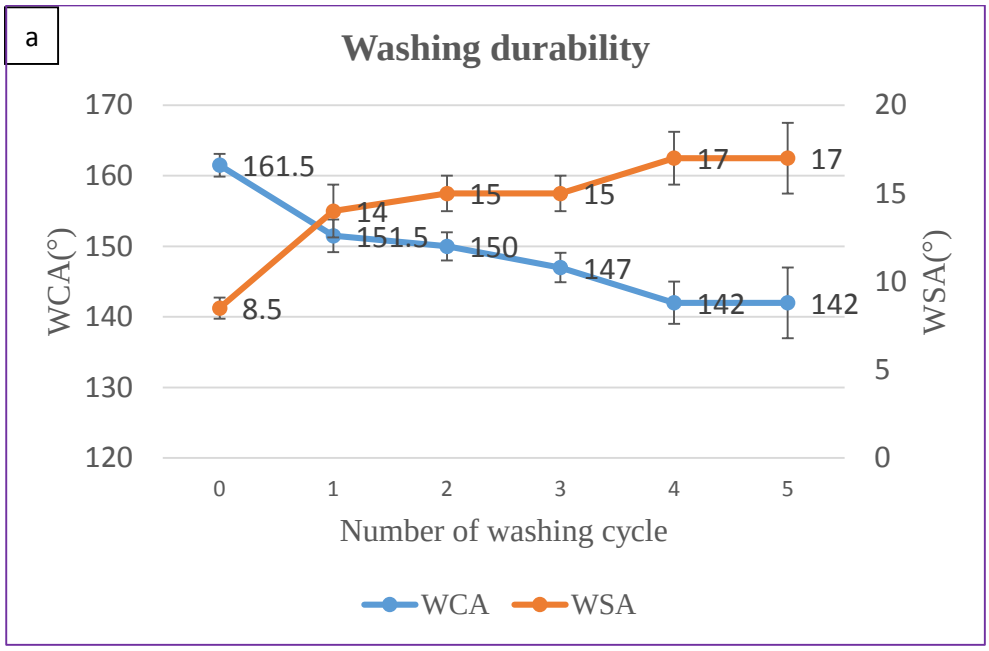

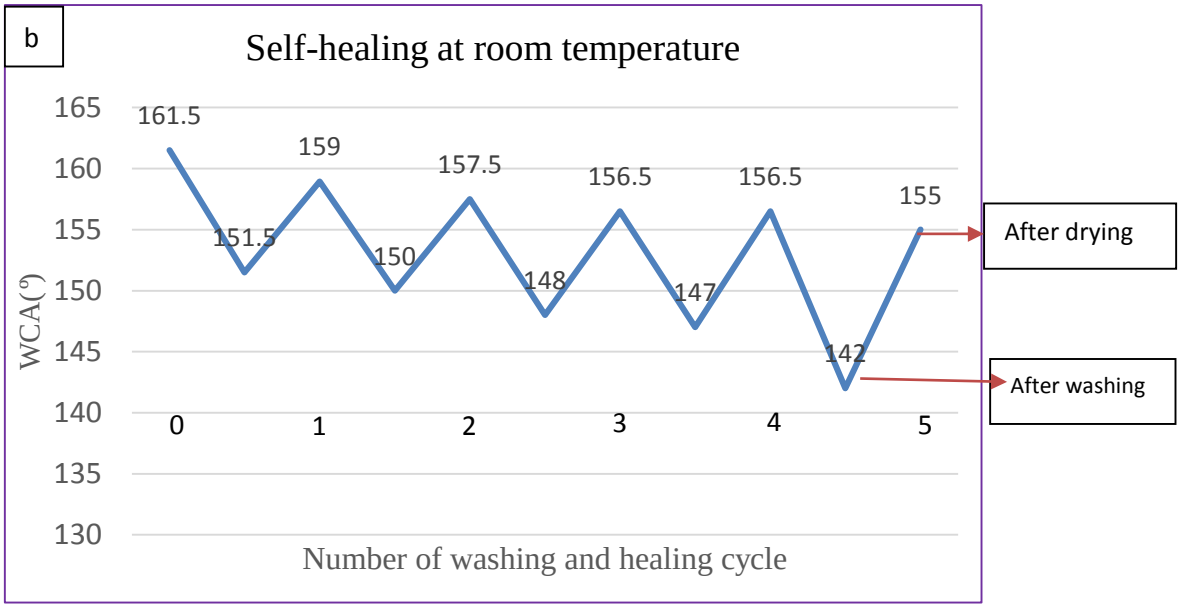

Figure 23. (a) Laundry washing test of treated cotton fabric for coating durability (b) self-healed at room temperature.

4.1.2 Adhesive tape and peel test

As already mentioned above, durability is a one of the important and basic requirements that extent product life span. Various methods were evaluated to be tested for durability of superhydrophobic coating materials. Usually tape test conducted as ASTM D3358 with a scotch Tape (810, 3M). In this study, we used adhesive tape commercial clothing tape cleaner (Scotch-Brite, 3M) to evaluate coating durability. After repeated tape peeled as 10,20,30,40 and 50 times, static contact angle and shedding angle were measured and evaluated. After 50 times of tape peeled it was maintained WCA 152.5º and WSA as 15º as figure 24. The reason of changing wettability is that, adhesive tape consisting of glues that's destroys nano-cluster (Nano structures) as worn off and sticky substances remained on the fabric surfaces thus effect of changing shedding angle dramatically. So even after 50 times of peel static contact angle maintained above 150º but shedding angle increased to 15º. Recently, same result was also reported by Wang et.al that coating surface was destroyed by multiple gluing and de-gluing of tape on the surface. [57].

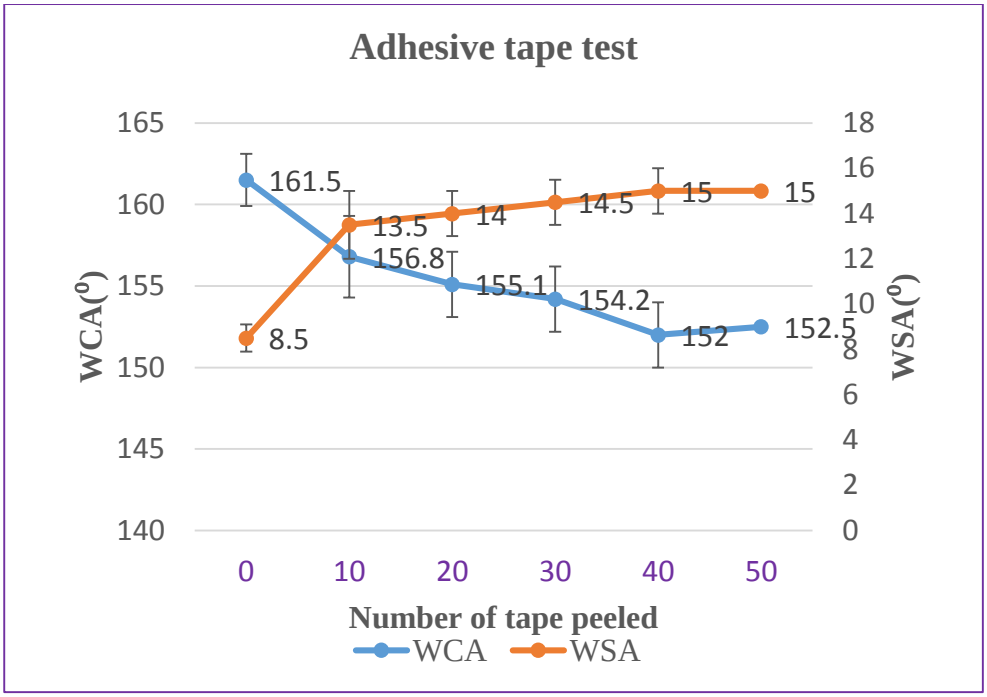

Figure 24. Adhesive tape peel test of treated cotton fabric for coating durability

4.2 Self- healing functionality of ODA/HDTMS treated fabric

4.2.1 Acid/alkali test

ODA is known as low surface energy materials and self-healing properties reported by many groups. Recently, self-healing superhydrophobic surface became interesting research area and many reports already have been done on these field [23,24]. Further study also be highly recommended due to its superb characteristics.

In this study, ODA/HDTMS as superhydrophobic coating materials. It was interesting that after coating treatments with waterborne ODA/HDTMS fabric showed self-healing properties after being damaged acid/alkali treatment. When treated fabric immerged acid/alkali solution for 15 min then rinsed by water and dry at room temperature it turned hydrophilic. But after dry 24h at room temperature or short time heating 100° C for 15 min, it restores its hydrophobicity (figure 25.)

To find out the reason of changing CA after acid/alkali treatment, acid leads to increase ODA on the surface and decrease HDTMS by damage alkyl chain of organosilanes or remove HDTMS from the surface. Thus, changing surface energy of the surface and results losing hydrophobicity. But after dry at room temperature 24h or short time heating long alkyl chain were reassembled due HDTMS migration thus restore hydrophobicity on the surface. For alkali, self-healing functionality found almost in same fashion as acid treated self-healing functions [52,58].

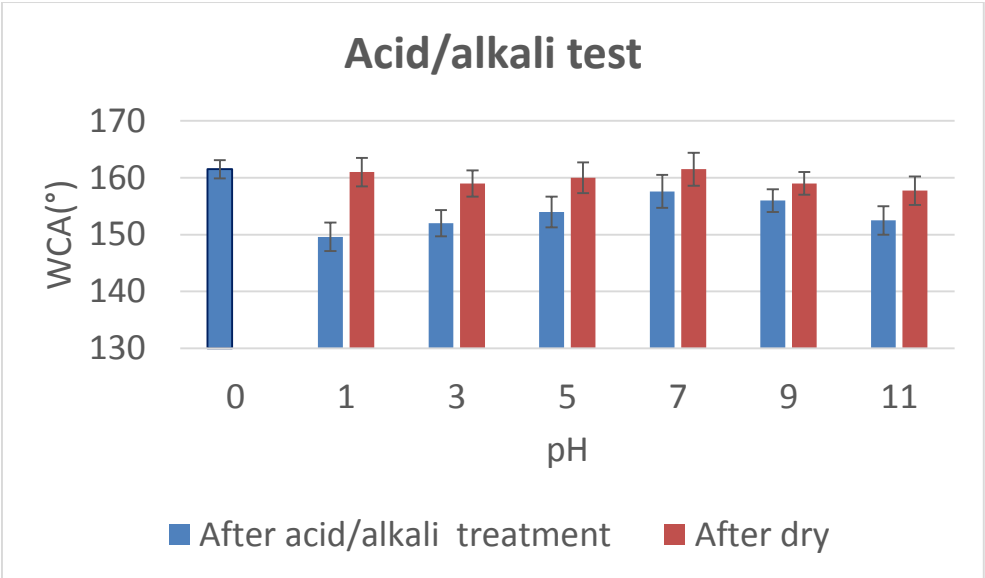

Figure 25. Acid/alkali test for self-healing properties of treated fabric in different pH level.

4.3 Breathable functionality of ODA/HDTMS treated fabric

4.3.1 Air permeability

The air permeability of the garment material measure how well air passing through garments passage and its very important for waterproof or superhydrophobic fabric. well air permeability maintains breathability and wearer comfort. In this study, we measured air permeability by an air permeability testing device (FX 3300, TEXTEST, Switzerland) under a pressure of 125 Pa. and expressed in units of cubic feet per minute (CFM). The untreated

sample (UT) and treated sample (OH_12) were compared and analyzed, and the results are shown in Figure 26. Sample UT was 40.06 CFM (cubic feet per minute), and treated sample air permeability was decreased to (OH_12) was 23.05. The reason of decreasing air permeability is possibly because after coating by ODA/HDTMS fabric surface covered by coating materials thus change pore size and thickness of the fabric.

The air permeability of the fabric depends on the amount of open pores determined by the aggregation state of the fibers, the structure of the fabric, materials, degree of thread twist, structure, thickness, etc. [59,60. Ogulata [61] showed that there is a linear positive correlation between pore size and air permeability, and if the porosity increased air permeability also increased.

As observed by SEM image, the surface was covered with ODA/HDTMS materials and the pores were covered with coating material thus air permeability is considered to be decreased.

4.3.2 Water vapor transmission rate

Water vapor transmission or moisture permeability of the clothing material is an ability to absorbs the water vapor that emitted from human body and it perform to transmit outside thus provide breathability and wearer comfort. The permeation is performed in

two ways. Direct permeation through the pores and moisture are absorbed and diffused from the inner surface of the fabric to the outer surface [62]. For breathable materials, when sweating, clothing prevents rising humidity and when the outside temperature is low, minimized condensation [63]. So, the moisture permeability is important factor and its related to the feeling of comfort and the burden of the human body. In this study we analyzed an untreated sample (UT) with treated sample (OH_12) and compare results are shown in Figure 26. According to the calcium chloride method of KS K 0594 (2015). Sample UT WVTR was 8613, and treated sample (OH_12) WVTR was slightly decreased to 8239 g/m^2.24h (gram per square meter a day). The reason of decreasing water vapor transmission rate is that after coating by ODA/HDTMS fabric surface covered by coating materials thus change pore size and thickness of the fabric. according to DTMS molecules blocked some pores by hydrophobic treatment [64]. On the other hand, Seoug et al. [65] reported that WVTR higher than 5000 g/m^2 a day is sufficient to feel comfort for wearer. From that, we found WVTR above 8000 g/m^2 and had excellent water vapor transmission, superhydrophobicity, and breathability.

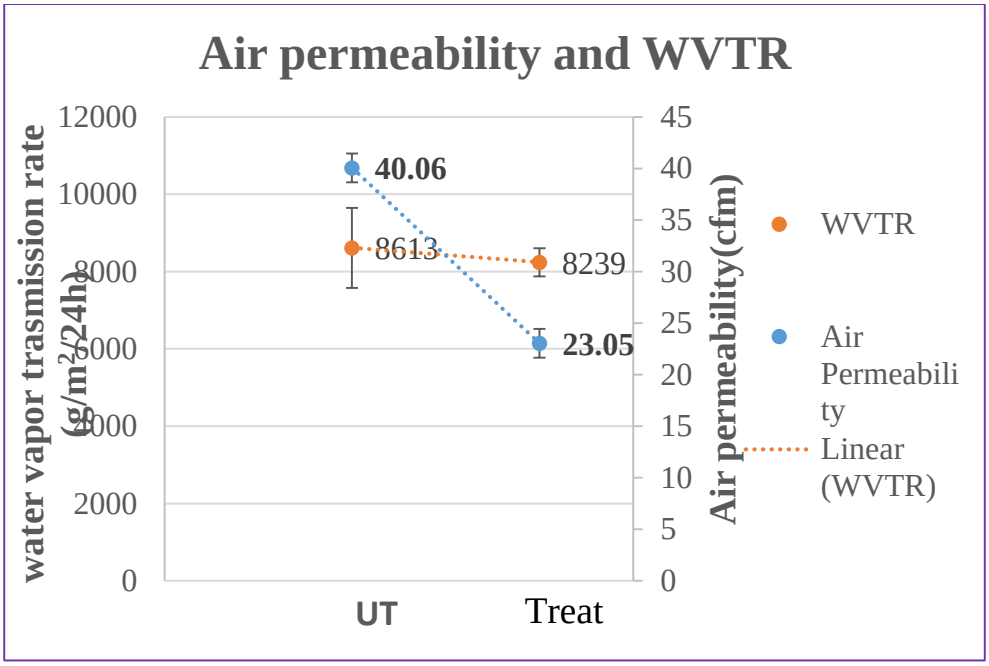

Figure 26. Air permeability and water vapor transmission rate(WVTR) of untreated and treated cotton fabric

Chapter 4. Conclusion

The aim of this study was to fabricate superhydrophobic cotton fabric from waterborne ODA and HDTMS coating by utilizing ODA to support formation of nanostructure with HDTMS hydrolytic organosilanes. Water contact angle and shedding angle were measured to identify superhydrophobicity of treated fabric. Surface morphology, chemical properties and functional group analysis were investigated by FE-SEM, XPS and FT-IR spectrum. Durability, self-healing properties, breathability were also evaluated. The summarized results are as follows.

1. In case of cotton surface treated with ODA only surface has still remaining smooth but cotton surface treated with HDTMS only surface roughness slightly increased. This is possibly because of strong Si-O-Si covalent bonding by hydroxyl group of cotton and hydrolytic silanes.
2. After ODA/HDTMS coating treatments cotton surface formed micro-nano scale roughness due to aggregated coating materials imparted on the fiber surface. By observing FE-SEM image ODA/HDTMS treated cotton surface hierarchical structured was observed and showed superhydrophobic static contact angle above 150° and shedding angle below 10°.

This is most possibly because of self-assembled ODA layer and HDTMS hydrolytic organosilanes.

3. Interestingly observed that, addition of HDTMS into the coating solution effects surface morphology thus increased hydrophobicity. And highest static contact angle, WCA 161.4±1.7° and shedding angle, WSA measured as 8.5±0.7° at ODA/HDTMS 1:2 molar ratios. It is also noted that, excess addition of HDTMS in the solution affect surface morphology resulting decreased hydrophobicity possibly because excess HDTMS disturbs aggregating and fills particle gaps.

4. Treated cotton fabric showed slightly decreasing of air permeability and water vapor transmission rate due to coating materials covered fabric surface thus reduced pore size. ODA/HDTMS treated fabric showed WVTR above 8000 g/m^2 x 24h that confirmed clothing breathability.

In summary, it was found that surface energy and surface roughness control by ODA/HDTMS molar ratio. And at ODA/HDTMS molar ratio 1:2 best superhydrophobicity was recorded as highest WCA 161.4±1.7° and lowest shedding angle, WSA as 8.5±0.7° . We envision that, this simple method to fabricate superhydrophobic surface from waterborne coating system and unique self-healing properties that can significantly prolong the lifespan of superhydrophobic cotton fabric in practical applications.

Limitation of this study: Total amount of ODA/ HDTMS were not same in this study. Highest total amount was 4 mol (for example ODA/HDTMS 3:1 or 1:3) so for the case of fabric treated with ODA alone or HDTMS alone it should be like 4:0 or 0:4. In this case surface morphology and other properties might have different for only ODA or HDTMS treated fabric.

Chapter 5. References

1. Pakdel, A.; Bando, Y.; Golberg, D. Plasma-Assisted Interface Engineering of Boron Nitride anostructure Films. ACS Nano 2014, 8, 10631-10639.
2. Choy, K. L. Chemical Vapour Deposition of Coatings. Prog. Mater. Sci. 2003, 48, 57-170.
3. Rao, N. P.; Tymiak, N.; Blum, J.; Neuman, A.; Lee, H. J.; Girshick, S. L.; McMurry, P. H.; Heberlein, J. Hypersonic Plasma Particle Deposition of Nanostructured Silicon and Silicon Carbide. J. Aerosol Sci. 1998, 29, 707-720
4. Lu, Y.; Ganguli, R.; Drewien, C. A.; Anderson, M. T.; Brinker, C. J.; Gong, W.; Guo, Y.; Soyez, H.; Dunn, B.; Huang, M. H.; Zink, J. I. Continuous Formation of Supported Cubic and Hexagonal Mesoporous Films by Sol-Gel Dip-Coating. Nature 1997, 389, 364-368.
5. Park, S., Kim, J., & Park, C. H. (2016). Analysis of the wetting state of super-repellent fabrics with liquids of varying surface tension. RSC Advances, 6(51), 45884-45893.
6. Kwon, S. O., Ko, T. J., Yu, E., Kim, J., Moon, M. W., & Park, C. H. (2014). Nanostructured self-cleaning lyocell fabrics with asymmetric wettability and moisture absorbency (part I). RSC Advances, 4(85), 45442-45448.

7. Wang,Z., Xu,Y., Liu, Y.,& Shao, L. (2015) A novel mussel-inspired strategy toward superhydrophobic surfaces for self-driven crude oil spill cleanup. J. Mater. Chem. A, 2015, 3,12171
8. Zhao, L., Liu, Q., Gao, R., Ang, J., Yang, Q., Liu, L. (2014) One-step method for the fabrication of superhydrophobic surface on magnesium alloy and its corrosion protection, antifouling performance. Corrosion Science 80 (2014) 177-183
9. Cao, L., Jones, A.K., Sikka, V.K., Wu, J., Gao, D. (2009) Anti-Icing Superhydrophobic Coatings. Langmuir 2009, 25(21), 12444-12448
10. Golovin, K. B.; Gose, J. W.; Perlin, M.; Ceccio, S. L.; Tuteja, A. Bioinspired Surfaces for Turbulent Drag Reduction. Philos. Trans. R. Soc., A 2016, 374, 0189.
11. Liu, K.; Zhang, M.; Zhai, J.; Wang, J.; Jiang, L. Bioinspired Construction of Mg–Li Alloys Surfaces with Stable Superhydrophobicity and Improved Corrosion Resistance. Appl. Phys. Lett. 2008, 92, 183103.
12. Husni, H.; Nazari, M. R.; Yee, H. M.; Rohim, R.; Yusuff, A.; Mohd Ariff, M. A.; Ahmad, N. N. R.; Leo, C. P.; Junaidi, M. U. M. Superhydrophobic Rice Husk Ash Coating on Concrete. Constr. Build. Mater. 2017, 144, 385–391.
13. Li, C.; Boban, M.; Snyder, S. A.; Kobaku, S. P. R.; Kwon, G.; Mehta, G.; Tuteja, A. Paper–Based Surfaces with Extreme

Wettabilities for Novel, Open-Channel Microfluidic Devices. Adv. Funct. Mater. 2016, 26, 6121-6131.

14. Lee, S. G.; Lee, D. Y.; Lim, H. S.; Lee, D. H.; Lee, S.; Cho, K. Switchable Transparency and Wetting of Elastomeric Smart Windows. Adv. Mater. 2010, 22, 5013-5017.

15. Zhang, X., Geng, T., Guo, Y., Zhang, Z., & Zhang, P. (2013) Facile fabrication of stable superhydrophobic SiO2/polystyrene coating and seperation of liquids with different surface tension. Chem. Eng. J., 231, 414-419 (2013). 61.

16. Hu,H., Gao, L., Chen, C.,& Chen, Q.(2014). Low-Cost, Acid/Alkaline-Resistant, and Fluorine-Free Superhydrophobic Fabric Coating from Onion like Carbon Microspheres Converted from Waste Polyethylene Terephthalate. Environ. Sci. Technol. 2014, 48, 2928-2933.

17. Yan, H., Zhou, Q., Wang, X., Chao, C.M., Tana, A.Y.X., & Xu, J. Engineering polydimethylsiloxane with two-dimensional graphene oxide for an extremely durable superhydrophobic fabric coating. RSC Adv., 2016, 6, 66834-66840.

18. Chen, K.; Zhou, S.; Yang, S.; Wu, L. Fabrication of All-Water Based Self-Repairing Superhydrophobic Coatings Based on UV Responsive Microcapsules. Adv. Funct. Mater. 2015, 25, 1035-1041.

19. Mates, J. E.; Schutzius, T. M.; Bayer, I. S.; Qin, J.; Waldroup, D. E.; Megaridis, C. M. Water-Based Superhydrophobic

Coatings for Nonwoven and Cellulosic Substrates. Ind. Eng. Chem. Res. 2014, 53, 222−227.

20. Ye, H.; Zhu, L.; li, W.; Liu, H.; Chen, H. Simple Spray Deposition of the Water−based Superhydrophobic Coatings with High Stability for Flexible Applications. J. Mater. Chem. A 2017, 5, 9882− 9890.

21. Schutzius, T. M.; Bayer, I. S.; Qin, J.; Waldroup, D.; Megaridis, C. M. Water−Based, Non−fluorinated Dispersions for Environmentally Benign, Large−Area, Superhydrophobic Coatings. ACS Appl. Mater. Interfaces 2013, 5, 13419−13425.

22. Wang, S.; Liu, K.; Yao, X.; Jiang, L. Bioinspired Surfaces with Superwettability: New Insight on Theory, Design, and Applications. Chem. Rev. 2015, 115, 8230−8293.

23. Liu, Q., Wang, X., Yu, B., Zhou, F. & Xue, Q. Self−healing surface hydrophobicity by consecutive release of hydrophobic molecules from mesoporous silica. Langmuir 28, 5845-5849 (2012).

24. Liu, Y. et al. One−Step Modification of Fabrics with Bioinspired Polydopamine@ Octadecylamine Nanocapsules for Robust and Healable Self−Cleaning Performance. Small 11, 426-431 (2015).

25. Liu, Y. et al. Mechanically induced self−healing superhydrophobicity. J. Phys. Chem. C 119, 7109-7114 (2015).

26. Liu, Y. et al. Accelerating the healing of superhydrophobicity through photothermogenesis. J. Mater. Chem. A 3, 17074-17079 (2015)
27. Lee, Y.L. Surface characterization of octadecylamine films prepared by Langmuir-Blodgett and vacuum deposition methods by dynamic contact angle measurements, Langmuir 15 (1999) 1796-1801
28. Yuan, J.J., Kimitsuka, N., & Jin R.H. Bioinspired Synthesis of a Soft-Nanofilament-Based Coating Consisting of Polysilsesquioxanes/Polyamine and Its Divergent Surface Control. ACS Appl. Mater. Interfaces 2013, 5, 3126-3133
29. Barthlott, W. and Neinhuis, C.; Purity of the sacred lotus, or escape from contamination in biological surfaces; Planta 1997, 202,1
30. Cao, Z., et al., Superhydrophobic pure silver surface with flower-like structures by a facile galvanic exchange reaction with [Ag(NH3)2] OH. Chem Commun (Camb), 2008(23): p. 2692-4.
31. BIXLER, G.D., & BHUSHAN, B. REVIEW. Biofouling: lessons from nature. Phil. Trans. R. Soc. A 370, 2381-2417
32. Gao, X.; Jiang, L. Biophysics: Water-Repellent Legs of Water Striders. Nature 2004, 432, 36-36.
33. Young, T. (1805). An essay on the cohesion of fluids. Philosophical Transactions of the Royal Society of London, 95, 65-87.

34. Wenzel, R. N., RESISTANCE OF SOLID SURFACES TO WETTING BY WATER. Industrial & Engineering Chemistry 1936, 28 (8), 988-994.
35. Cassie, A. B. D.; Baxter, S., Wettability of porous surfaces. Transactions of the Faraday Society 1944, 40 (0), 546-551.
36. L. Feng, Y. Zhang, J. Xi, Y. Zhu, N. Wang, F. Xia and L. Jiang. Petal Effect: A Superhydrophobic State with High Adhesive Forc. Langmuir, 2008, 24, 4114.
37. B. Bhushan and E. K. Her. Fabrication of Superhydrophobic Surfaces with High and Low Adhesion Inspired from Rose Petal.Langmuir, 2010, 26, 8207.
38. B. Bhushan and M. Nosonovsky, The rose petal effect and the modes of superhydrophobicity. Philos. Trans. R. Soc., A, 2010, 368, 4713
39. Furmidge, C. G. L., Studies at phase interfaces. I. The sliding of liquid drops on solid surfaces and a theory for spray retention. Journal of Colloid Science 1962, 17 (4), 309-324.
40. Sun, M.; Luo, C.; Xu, L.; Ji, H.; Ouyang, Q.; Yu, D.; Chen, Y., Artificial Lotus Leaf by Nanocasting. Langmuir 2005, 21 (19), 8978-8981.
41. Park, S., Kim, J., Park, C.H. (2016). Influence of micro and nano-scale roughness on hydrophobicity of a plasma-treated woven fabric. Textile Research Journal2017, Vol. 87(2) 193-207.

42. Ming, W.; Wu, D.; van Benthem, R.; With, G. d., Superhydrophobic films from raspberry-like particles. Nano letters 2005, 5 (11), 2298-2301.
43. Artus, G. R. J.; Jung, S.; Zimmermann, J.; Gautschi, H.-P.; Marquardt, K.; Seeger, S. Silicone Nanofilaments and Their Application as Superhydrophobic Coatings. Adv. Mater. 2006, 18, 2758-2762.
44. Elsaesser, A,. & C. Vyvyan Howard, C. V. Toxicology of nanoparticles. Advanced Drug Delivery Reviews 64 (2012) 129-137
45. Oberdorster, G,. & Utell, M.J. Ultrafine particles in the urban air: to the respiratory tract—and beyond? Environ. Health Perspect. 110 (2002) A440-A441
46. Park, H. & Grassian, V.H. Commercially manufactured engineered nanomaterials for environmental and health studies: important insights provided by independent characterization, Environ. Toxicol. Chem. 29 (2010) 715-721.
47. Brown, S.C,. Palazuelos, M,. Sharma, P,. Powers, K.W,. Roberts, S.M,. Grobmyer, S.R,. & Moudgil, B.M. Nanoparticle characterization for cancer nanotechnology and other biological applications, Methods Mol. Biol. 624 (2010) 39-65
48. Lindstrom, A.B,. Strynar, M.J,. & Libelo, L.E. Polyfluorinated Compounds: Past, Present, and Future. Environ. Sci. Technol. 2011, 45, 7954-7961

49. Zimmermann, J., Seeger, S., & Reifler, F. A. (2009). Water shedding angle: a new technique to evaluate the water-repellent properties of superhydrophobic surfaces. Textile Research Journal, 79(17), 1565- 1570.
50. ASTM D737-04(2016), Standard test method for air permeability of textile fabrics.
51. KS K 0594(2015), Test method for water vapour permeability of textiles.
52. Wang, H,. Zhou, H,. Liu, S,. Shao, H,. Fu, S,. Rutledge G.C& Lin, T. Durable, self-healing, superhydrophobic fabrics from fluorine-free, waterborne, polydopamine/ alkyl silane coatings. RSC Adv., 2017, 7, 33986
53. J. H. Yim, V. Rodriguez, A. A. Williams and J. K. Hirvonen, Surf. Coat. Technol., 2013, 234, 21-32.
54. I. Woodward, W. C. E. Scho eld, V. Roucoules and J. P. S. Badyal, Langmuir, 2003, 19, 3432-3438.
55. X. Wang, S. Xu, Y. Tan, J. Du and J. Wang, Carbohydr. Polym., 2016, 140, 188-194.
56. Yang, J,. Zhang, Z,. Xu, X,. Zhu, X,. Men, X,. & Zhou, X. Superhydrophilic-superoleophobic coatings. J. Mater. Chem., 2012, 22, 2834-2837
57. Wang, N.; Xiong, D.; Deng, Y.; Shi, Y.; Wang, K. Mechanically Robust Superhydrophobic Steel Surface with Anti-Icing, UV-Durability, and Corrosion Resistance Properties. ACS Appl. Mater. Interfaces 2015, 7, 6260-6272.

58. Xue, C.H., Robust, Self-Healing Superhydrophobic Fabrics Prepared by One-Step Coating of PDMS and Octadecylamine
59. Bagherzadeh, R., Montazer, M., Latifi, M., Sheikhzadeh, M., & Sattari, M. (2007). Evaluation of comfort properties of polyester knitted spacer fabrics finished with water repellent and antimicrobial agents. Fibers and Polymers, 8(4), 386-392.
60. Ogulata, R. T. (2006). Air permeability of woven fabrics. Journal of Textile and Apparel, Technology and Management, 5(2), 1-10.
61. Oğulata, R. T., & Mavruz, S. (2010). Investigation of porosity and air permeability values of plain knitted fabrics. FIBRES & TEXTILES in Eastern Europe, 18(5), 71-75
62. 김성련, "피복재료학", 파주: 교문사, 2009
63. 김은애, & 유신정. (2004). 투습방수 소재 및 평가 기술. Fiber Technology and Industry, 8(3), 271.
64. Kang, M., et al., Preparation of superhydrophobic polystyrene membranes by electrospinning. Colloids and Surfaces A: Physicochemical and Engineering Aspects, 2008. 313-314: p. 411- 414.
65. Park, S.K, K.D.K., Kim, H.T. Preparation of silica nanoparticles determination of the optimal synthesis conditions for small and uniform particles.

국 문 초 록

옥타데실아민/알킬 실레인 수분산 코팅을 통한 초소수성 면 직물 개발

라만

의류학 및 의류소재연구실

서울대학교 대학원

최근 초소수성 표면은 광범위한 적용성 및 다기능성 덕에 고급 직물 처리를 비롯한 직물과 비직물 분야 모두에서 주목 받는 연구분야이다. 그에 따라 초소수성 표면을 구현하기 위해 일반적인 물질들을 사용하여 표면 거칠기와 표면 에너지를 조절하는 많은 방법이 적용되고 있다. 하지만 많은 경우, 매우 유독한 유기 용매가 사용되고 있으며, 기능의 낮은 내구성, 가격, 복잡한 공정 등의 문제가 있어 초소수성 직물이 일상 생활까지 적용되기 까지는 아직 무리가 있다. 그렇기에, 초소수성 표면 구현시 제작이 쉽고, 내구성이 있으며, 자가회복이 가능한 방법을 개발하는 것이 필요하다. 따라서 본 연구에서는 물을 용매로 하여 알킬 아민 마이크로-나노 구조를 형성하는데에 HDTMS 의 가수분해 다중축합(hydrolytic polycondensation)에 의한 꽃잎 혹은 그물망 형태 나노구조의 형성을 위해 자기조립된 ODA 단분자층을 촉매로 활용하여 내구성 다기능성 초소수성 표면을 구현하는 간단한 공정을 개발하는데에 목적을 두었다. 직물에서 널리 사용되는 셀룰로오스 면 직물을 시료로 선정했으며, 많은 수산화기를 가지는 면의 특성을 활용하여 뭉쳐진 ODA/HDTMS 마이크로-나노 피브릴과 Si-O-Si 의 강력한 공유 결합을 형성하여 이어지도록 하였다.

ODA 와 HDTMS 의 농도에 따른 영향을 알아보기 위해, 표면구조와 화학적 조성을 각기 다른 몰비율에 따라 알아보았다. 표면 구조는 전계방출 주사전자현미경(FE-SEM)을 고배율(nm 단위)로 확인하였다. 화학적 조성은 푸리에 변환 적외분광법 분광광도계(FT-IR)와 X-선 광전자 분광법(XPS)를 사용하여 코팅된 물질이 섬유 표면에 성공적으로 코팅 되었는지 확인하였다. 표면 젖음성은 증류수의 정적 접촉각과 기울임각(shedding angle)을 통해 측정하였다. 기능의 내구성과 자가회복 성능, 투습도, 공기투과도 역시 검사하였다. 면직물을 ODA 로만 코팅하였을 경우 ODA 가 양쪽 친매성(amphiphilic) 물질이기 때문에 마이크로-나노 거칠기는 생기지 않았다. 하지만 면직물을 HDTMS 로만 코팅하였을 때에는, 거칠기는 나타나지 않았지만 소수성 표면이 구현되었다. 이는 HDTMS 가 면의 셀룰로오스의 수산화기와 그래프트 하여 미끄러운(slippery) 표면을 만들기 때문이다. 흥미롭게도, 면직물이 ODA/HDTMS 혼합액에 딥코팅 되었을 때 마이크로-나노 단위의 거칠기가 형성되었다. ODA/HDTMS 의 몰비율이 3:1 에서 1:2 비율로 갈수록 표면은 더 거칠어졌으며, 정적 접촉각 150° 이상과 물의 기울임각 10° 미만이 얻어졌다. 초소수성의 최적조건은 ODA/HDTMS 의 몰비율이 1:2 일 때 얻어졌는데, 가장 낮은 물의 정적 접촉각 161.4±1.6 도와 가장 낮은 물의 기울임각 8.5±0.7° 가 얻어졌다. 본 연구는 간단한 일 단계 딥 코팅 방법으로 biosilicificaition 용매 시스템을 통해 표면에너지를 낮추고 마이크로-나노 거칠기를 구현하여 초소수성을 얻었다는 기여점을 가진다.

주요어: 초소수성, ,자가회복, Biosilicification,비불소계 소재, 딥코팅

학 번: 2016-26765